

Original Article

Effect of intra-articular hyaluronan injection on inflammation and bone remodeling in the epiphyses and metaphyses of the knee in a murine model of joint injury

Quan Shen^{1*}, Jun Li^{1*}, Deva Chan², John D Sandy³, Jun Takeuchi⁵, Ryan D Ross^{3,4}, Anna Plaas¹

¹Department of Internal Medicine (Rheumatology), Rush University Medical Center, Chicago, IL, USA; ²Department of Biomedical Engineering Rensselaer Polytechnic Institute, Troy, NY, USA; Departments of ³Orthopedic Surgery, ⁴Cell & Molecular Medicine, Rush University Medical Center, Chicago, IL, USA; ⁵Medical Science Liaison Unit, Seikagaku Corporation, Tokyo, Japan. *Equal contributors.

Received September 18, 2018; Accepted December 26, 2018; Epub June 15, 2019; Published June 30, 2019

Abstract: The TTR (transforming growth factor β 1 (TGF β 1) injection with treadmill running) model of murine joint injury was used to examine effects of intra-articular Hyaluronan (IA HA) on the metabolism of subchondral bone. HA was injected 24 h after TGF β 1 injection and its effects on the mRNA of 80 genes in the Nfkb pathway, and bone remodeling genes, *Acp5*, *Nos2* and *Arg1*, in femoral and tibial epiphyses/metaphyses of injected and contralateral legs was assessed. Structural bone parameters at those sites were determined by Micro-computed tomography (micro CT) and bone remodeling cells identified with histochemistry for tartrate-resistant acid phosphatase and immunohistochemistry for Nitric oxide synthase 2 (NOS2) and Arginase 1. Gene expression responses in femoral compartments were generally inhibitory and notably biphasic whereas the tibia was relatively non-responsive. Gene expression was also altered in the contralateral femoral compartment but were predominantly activated. IA TGF β 1 did not alter bone structure in the injected leg, but resulted in a statistically significant reduction (25-40%) in trabecular bone of the contralateral limb. IA HA did not affect such changes. This bone loss was associated with an acute decrease in transcript abundance for *Acp5*, *Nos2*, *Arg1* and this decrease persisted for *Nos2* and *Arg1*. In conclusion, the data illustrate that in this model, IA TGF β 1 injection results in marked biphasic changes in Nfkb-regulated apoptosis, IL1 and IL12 pathways, which were transiently altered after IA HA therapy. The finding that all modulations are essentially restricted to the femoral compartment is consistent with the predominant localization and clearance of injected HA from this site.

Keywords: TGF β 1, hyaluronan, inflammation, Nfkb, bone, macrophages

Introduction

Hyaluronan (HA) is increasingly used in a wide range of therapeutic applications, including musculoskeletal tissue regeneration and pain management [1]. Although some evidence has been published for pre-clinical clinical efficacy of local HA therapy for joint diseases with an inflammatory component, such as post-traumatic osteoarthritis [2-5], the dosage (single vs multiple), the timing and location of the injections have yet to be optimized. IA (Intra-Articular) HA injections have also been used to treat cartilage lesions following surgical micro

fracture [6] but the results have been inconclusive [7, 8].

We and others have studied the effects of IA HA injections in rodent and rabbit models of OA. For example, a single dose of high molecular weight HA has a protective effect against local tissue changes and also against early pain sensitization in the TTR (TGF β 1 injection with treadmill running) [9] and the DMM models of OA [10]. In addition, HA alone [11] or in combination with PRP [12] or dexamethasone [13] activates chondrogenic genes in the cartilage/subchondral bone and represses fibrogenic genes

throughout the joint in murine OA, with similar findings reported in a lapine OA model [3]. In a recent study, Duane et al [14], using a mechanical overload model of knee joint tissue degeneration, reported that IA injection of an HA derivative did not affect structural changes in cartilage or synovium, and produced only minor effects on femoral epiphyseal bone remodeling.

Because of its widespread biomedical usage it has become imperative to understand the various biological activities of the molecule (in its multiple formulations) and a recent paper [15] has highlighted the well-documented role of HA in inflammatory environments. However, whether exogenously supplied HA acts as an anti- or pro-inflammatory in different phases of the inflammatory responses to tissue injury is unknown [16].

In the context of using IA HA formulations for therapeutic intervention in correcting remodeling of various tissue in the OA joint, it should be noted that in addition to the soft tissues, this includes the epiphyseal/subchondral bone [17-20] and the marrow [21]. However, there is currently no information on the effect of HA on inflammatory pathways and remodeling of the epiphyseal bone that accompany OA progression.

Our current studies using the TTR model were motivated by the knowledge that the transforming growth factor (TGF)- β super family are important regulators in osteoclastogenesis with Smad-mediated signaling being crucial for inducing osteoclast differentiation. TGF β 1 induced inflammation through activation of the Nfkb pathway [22] can lead to abnormal bone remodeling that results in long term bone-loss when this pathway is chronically modulated [23, 24]. Moreover, when injected into the knee joint of mature mice this growth factor initiates extensive intra-articular osteophyte formation [25, 26], and it has been suggested that via its induction of NGF production [27], it can be an important inducer of osteoarthritic pain.

We report here studies using the TTR model, on the effect of IA HA on TGF β 1 induced changes in expression levels of 73 genes in the Nfkb pathway, osteoclast/osteoblast specific genes, as well as macrophage specific markers, *Nos2* and *Arg1*, in the tibial and femoral epiphyses. Bone quality of epiphyseal, metaphyseal and cortical regions of the femur and tibia were

evaluated and osteoclast/macrophage [28, 29] in these regions were identified using tartrate-resistant acid phosphatase (TRAP) histochemical staining and IHC for NOS2 and Arginase 1.

Our data show that in the TTR model, IA HA acutely altered TGF β 1 induced changes in Nfkb pathway and bone metabolism gene expression, primarily in the femoral epiphyses of TGF β 1 injected knees. We also observed significant activation of Nfkb pathway genes in contralateral joints, and this response was amplified after the HA injection. TGF β also resulted in rapid trabecular bone loss in the femoral metaphyses, but only in the contralateral knee, and this was not modified by IA HA. Together these data support the conclusion that a single IA HA injection can serve as a transient anti-inflammatory agent in soft tissues [9] through its modification of transcriptional regulation of genes in the NfKb pathway, but that it has no detectable effects on epiphyseal or metaphyseal bone structural parameters in either injected or contralateral knees.

Materials and methods

In vivo murine studies

The murine TTR model is described in detail elsewhere [9, 10]. Male mice (wild type C57BL/6 background, age 12 weeks) were bred in-house, and all animal protocols were approved by the Rush University Medical Center Animal Care and Use Committee. Therapeutic HA (Supartz FX™, Seikagaku Corporation) or saline injections were given one day after the second TGF β 1 injection. Control groups included mice subjected to treadmill running only for 1 week or 3 weeks, as well as age-matched cage maintained mice. A summary of experimental groups and mice used for each of the outcomes is given in [Table S1](#).

QPCR gene expression assays

Femoral and tibial epiphyseal/metaphyseal samples were isolated after joint separation by removal of all fibrous tissues (menisci, ligament etc.) and sharp linear dissection at the metaphyseal interface with the growth plates before storage at -20°C in RNALater (Life Technologies, Carlsbad, CA). On inspection under the dissecting microscope, these samples reproducibly contained the complete articular surfaces and epiphyseal bone along with the majority of the growth plate cartilages with attached spicules

Therapeutic hyaluronan and bone remodeling in osteoarthritis

of metaphyseal bone and the bone marrow. RNA was prepared either from a pool of three or individual epiphyseal samples as described in [Table S1](#). Briefly, tissues in RNALater were thawed on ice, rinsed with fresh RNALater (Qiagen, Valencia, CA, USA), snap-frozen in liquid nitrogen and pulverized. RNA purification and cDNA synthesis was performed as previously described as described in [9]. RT² Profiler PCR Array (Qiagen) plates were used to quantify transcript abundance for Nfkb Pathway genes (PAMM-025Z, see [Figure S1](#) for gene listing and baseline Δ Ct values). Transcript abundance of bone anabolic and catabolic genes was also determined using Taqman®-primers *Alpl*, Mm00475834_m1; *Bglap*, *Bglap3*, *Bglap2*, Mm03413826_mH; *Acp5*, Mm00475698_m1; *Ctsk*, Mm00484039_m1; *Tnfsf11*, Mm00441906_m1; *Tnfrsf11b*, Mm00435454_m1, *Nos2*, Mm00440502_m1 and *Arg1*, Mm00475988_m1. The Δ Ct = [Ct (gene of interest)-Ct (Gapdh)] and Ct>35 considered 'non-detectable' (ND) was used to compute treatment-induced fold-change in expression as $2^{-\Delta\Delta$ Ct, where $\Delta\Delta$ Ct = [Δ Ct (post-injury time point) - Δ Ct (naïve)], with only ≥ 1.9 fold increase or decrease considered biologically significant.

Bone micro CT analyses

Distal femurs and proximal tibias from all experimental groups were imaged with a SCANCO μ CT40 desktop scanner at an isotropic spatial resolution of 12 μ m, an operating voltage of 55 kVp, a current of 145 μ A, and an integration time of 300 ms. Trabecular bone volumes of interest were semi-automatically segmented at the endocortical boundary in the metaphysis and diaphysis ([Figure S3](#)) with on-board software, which was then used to estimate bone volume fraction (BV/TV), and trabecular bone parameters of number (Tb.N), thickness (Tb.Th), and spacing (Tb.Sp). Cortical bone volumes of interest were similarly segmented for estimation of cortical bone parameters. All data are expressed as fold changes relative to age-matched cage control groups ([Table S2](#)).

Histology and immunohistochemistry

Knee joints (n=3 per experimental group) were processed as previously described. Briefly, joints were fixed in formaldehyde, decalcified in EDTA, processed, embedded in paraffin, and 5 μ m thin sagittal sections cut through the entire

joint. Sections (n=36) from the mid-portion of each specimen, were used for immunohistochemistry: Sections (n=6 per antibody) were de-paraffinized and incubated overnight at 4°C with the following probes: anti NOS2 (1 μ g/mL [Thermo Scientific, PA3-030A]) or anti-Arginase 1 (1 μ g/mL, [Bioss, bs-8585R]), followed by biotinylated anti-rabbit IgG as secondary antibody. All sections were counterstained with methyl green. Negative control staining is shown in [Figure S2](#).

To identify osteoclast-like cells in sections of injected and contralateral knee joints, formalin-fixed, EDTA-decalcified and paraffin embedded sections were stained using the SIGMA-Aldrich Diagnostics Acid Phosphatase, Leukocyte (TRAP) kit. Staining was carried out as per manufacturer's protocol and sections were counterstained with 0.05% Fast Green.

Statistical analysis

Statistical analysis was performed using SPSS (version 17, IBM). Data was first tested for normality using a Shapiro-Wilk test. All data was normally distributed and therefore group effects were assessed using a one-way analysis of variance (ANOVA). If significant, specific between group comparisons were made using a Tukey post-hoc test.

Results

The TTR model has disparate effects on Nfkb pathway gene expression in femoral and tibial epiphyses of injected legs

The effect of the TTR model on the expression of 73 genes in the Nfkb pathway, measured in epiphyses at different times post-injection, for both injured and contralateral legs, is shown in [Figure 1](#) (heatmap) and [Table S3](#) (numerical data). Genes are listed in 8 functional groups (as per Qiagen) and data is presented as increased or decreased fold-change relative to values obtained for UI (uninjured) age-matched tissue samples. The validity of the fold change data is based on the high reproducibility of expression (as Δ Ct values) of individual genes in biological replicates. Assays of Pools 1, 2 and 3 ([Figure S1](#)) show that for naïve joints the three results for the femoral (FE) or tibial (TE) samples always varied by less than 1.0 Δ Ct unit from the mean value which was used for the fold-activation calculation in [Figure 1](#).

Therapeutic hyaluronan and bone remodeling in osteoarthritis

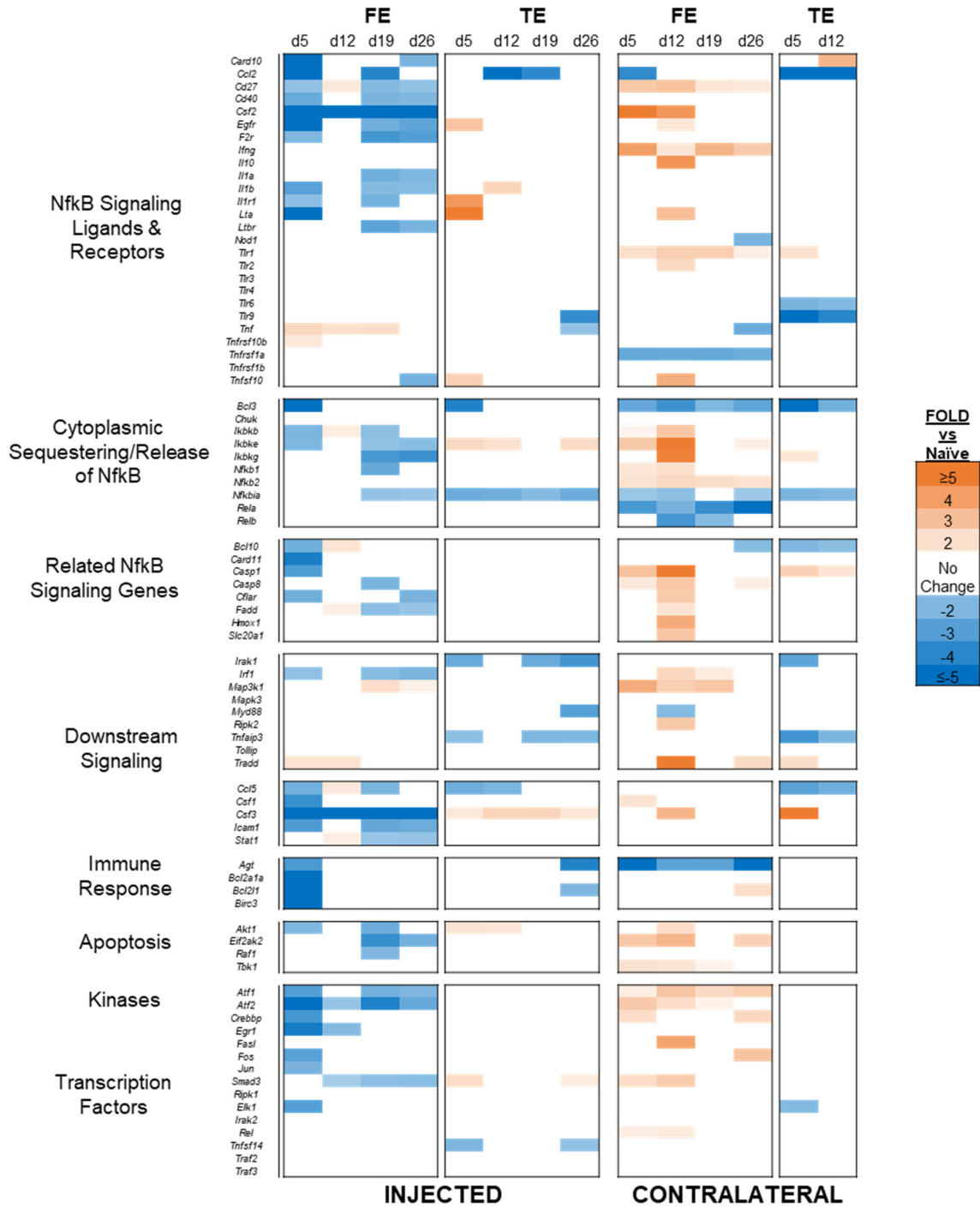


Figure 1. Heatmap illustration of fold changes vs UI in relative mRNA abundance for Nfkb pathway genes in femoral and tibial epiphyses in the TTR model. Colored boxes are only shown for statistically significant ($P < 0.05$) fold changes relative to naïve levels.

The response to the TTR model (**Figure 1**) was distinctly different in the femoral vs the tibial epiphyses. In the femoral epiphysis of the injured knee, the apparent mRNA abundance of 50/73 genes was significantly ($P < 0.05$) altered from naïve levels at one or more time points

and most strikingly, the injured femur responded biphasically with a generalized inhibition of expression (46/50 genes) on day 5, which was normalized by day 12 but re-established on days 19 and 26 for most genes. Relative to the generalized femoral response, very limited

Therapeutic hyaluronan and bone remodeling in osteoarthritis

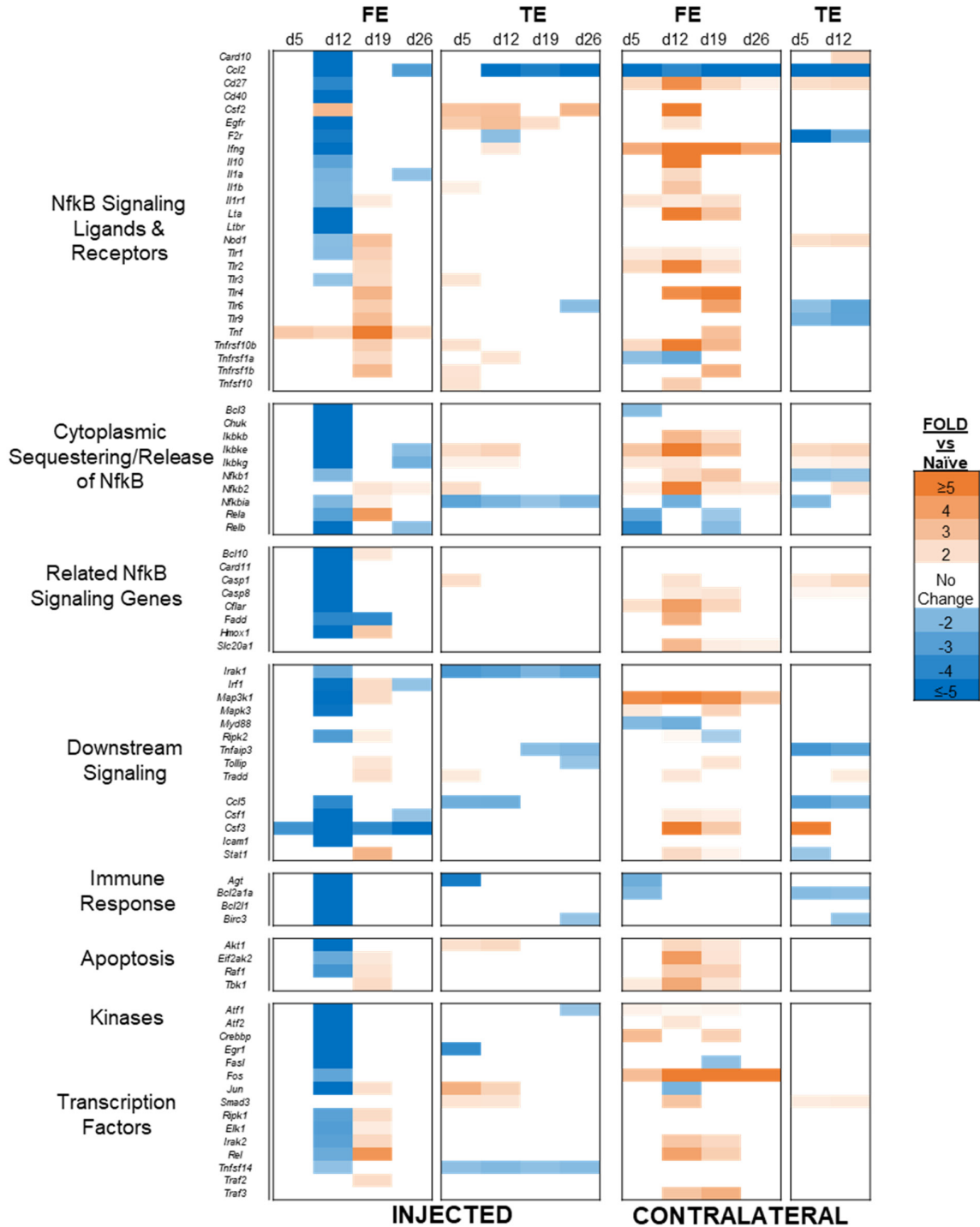


Figure 2. Heatmap illustration of IA HA-induced fold changes vs UI in relative mRNA abundance for Nfkb pathway genes in femoral and tibial epiphyses in TTR model. Colored boxes are only shown for statistically significant ($P < 0.05$) fold changes relative to naïve levels.

changes were seen in the tibial epiphysis, with only 23/73 genes affected (11 inhibited and 12 activated), and (perhaps more notably) where the same gene was altered in both epiphyses (18 genes) the change in expression

was often (9 genes) a femoral inhibition and a tibial activation. When taken together, these results showed that, despite the intra-articular location of the injections and the similarities in tissue structure and anatomic location, the

Therapeutic hyaluronan and bone remodeling in osteoarthritis

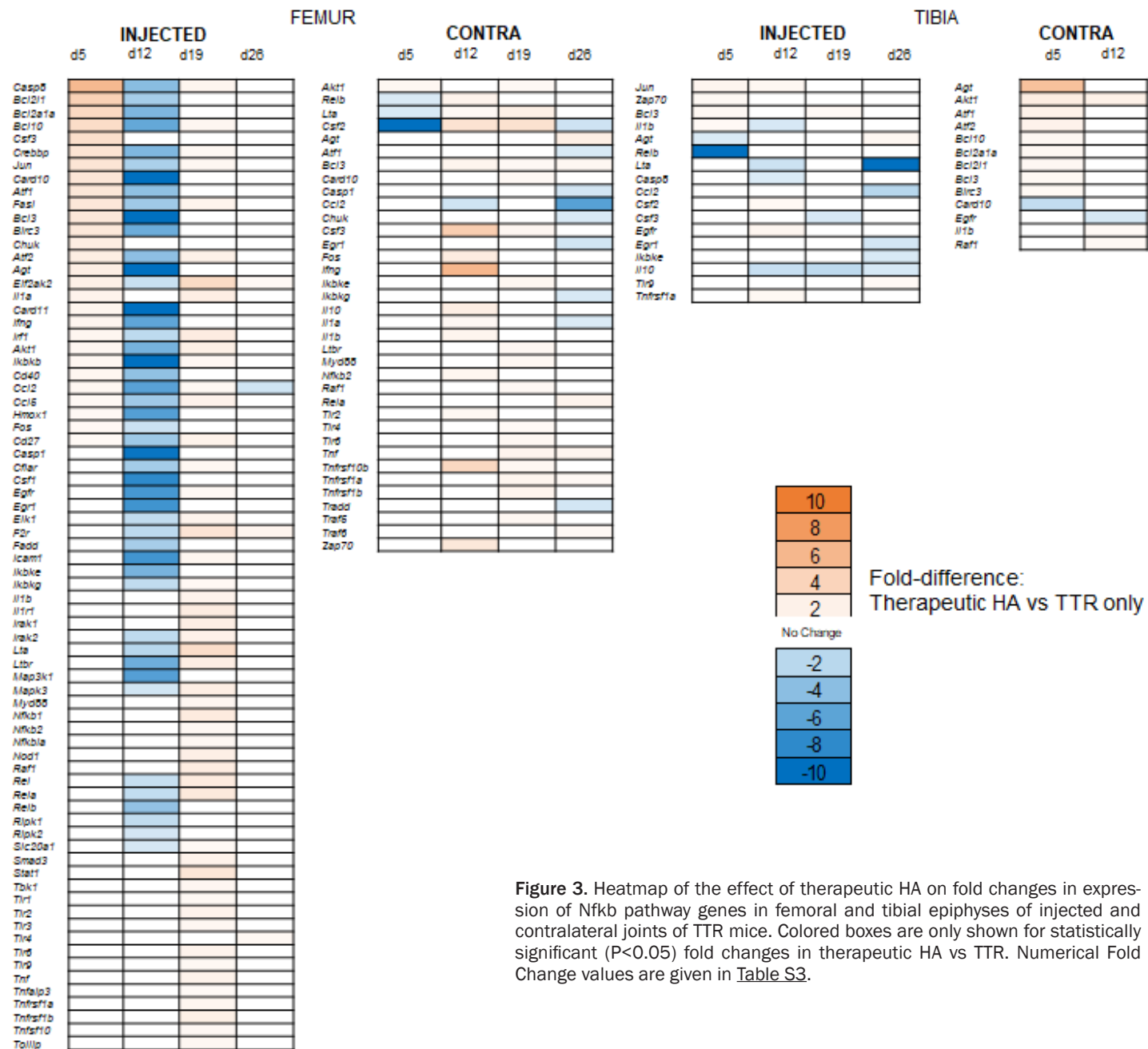


Figure 3. Heatmap of the effect of therapeutic HA on fold changes in expression of Nfkb pathway genes in femoral and tibial epiphyses of injected and contralateral joints of TTR mice. Colored boxes are only shown for statistically significant ($P < 0.05$) fold changes in therapeutic HA vs TTR. Numerical Fold Change values are given in Table S3.

Therapeutic hyaluronan and bone remodeling in osteoarthritis

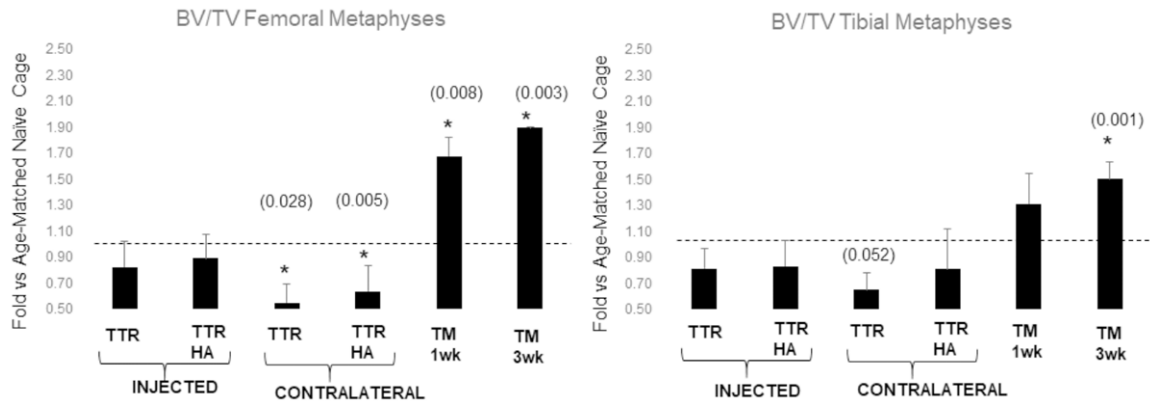


Figure 4. Alterations in metaphyseal and epiphyseal BV/TV after TTR, TTR+HA and TM treatments. Injected and Contralateral legs were analyzed separately for the TTR or TTR+HA groups. *Statistical significance was calculated using 1-way Nova software and number of animals analyzed for each group is given in [Table S1](#). NS=P>0.05. Data are expressed relative to UI (for TTR ± HA) or Cage (for TM) age matched controls.

signaling response to joint injury was quite distinct on the femoral and tibial aspects of the joint. In fact only 6/73 genes (*Ccl2*, *Bcl3*, *Nfkb1a*, *Ccl5*, *Agt* and *Bcl2l1*) showed the same response in both tibia and femur, which was an inhibition.

The TTR model has opposite effects on NFkb pathway gene expression in femoral epiphyses of injured and contralateral legs

In addition to the focal nature of the response in the femur of the injected joint, there was also an unexpectedly robust response in the contralateral femoral epiphyses (44/73 genes) suggesting that femoral epiphyseal cells were more responsive than tibial cells in general (**Figure 1**). However, in contrast to the injected side where expression was generally inhibited in the femur, the majority (33/44) of affected genes in the contralateral femur were activated, consistent with secondary signaling via a circulating non-TGFβ1 factor. Further, consistent with only 23/73 genes being affected in the tibia of the injected joint, only 16/73 were affected in the contralateral tibia.

Therapeutic HA markedly affects Nfkb1 pathway gene expression in the femoral epiphysis of the injured joint in the TTR model

A single IA HA dose delayed the generalized inhibition of expression seen in contralateral femurs from day 5 (**Figure 1**; [Table S2](#)) to day 12 (**Figure 2**). More remarkably perhaps, therapeutic HA essentially eliminated the late stage (days 19/26) inhibitions (**Figure 1**) and instead

caused activation, particularly on day 19 (**Figure 2**). These marked effects of HA were not the result of a joint “wash-out” effect by the HA solution since when saline was used instead of HA no significant changes occurred in gene expression as a result of the injection ([Figure S2](#)).

We next calculated the fold-change effects of HA injection (TTR+HA vs TTR) from ΔCt values, and this data is shown in **Figure 3** and [Table S3](#), where only genes exhibiting some sensitivity to HA are provided. Most apparent was the finding on the femoral side that similar to TGFβ1, the HA effect was also phasic with a set of 25 genes (*Casp8*, *Bcl2l1*, *Bcl2a1a*, *Bcl10*, *Crebbp*, *Jun*, *Card10*, *Atf1*, *Fasl*, *Bcl3*, *Birc3*, *Atf2*, *Agt*, *Eif2ak2*, *Card11*, *Ifng*, *Irf1*, *Akt1*, *Ikbkb*, *Cd40*, *Ccl2*, *Ccl5*, *Hmox1*, *Fos*, *Cd27*) which were activated by the HA at day 5, inhibited at day 12 and re-activated at day 19. The other 49 genes were unaffected by HA on day 5 and subsequently were unaffected or inhibited on day 12 and generally activated on day 19. A 14-gene subset (*Cflar*, *Egfr*, *Elk1*, *F2r*, *Icam1*, *Ikbkg*, *Irak2*, *Lta*, *Ltbr*, *Map3k1*, *Mapk3*, *Rel*, *Rela*, and *Slc20a1*) of the 49 genes responded in concert, in that they were unaffected on day 5, inhibited on day 12, activated on day 19 and unaffected on day 26.

Effect of the TTR model on structural bone parameters

Micro CT analysis for four structural parameters was done on injected and contralateral legs from four mice of each of the three treat-

Therapeutic hyaluronan and bone remodeling in osteoarthritis

Table 1. Changes in metaphyseal trabecular bone properties following TTR, TTR+HA and TM treatments

Parameter	TTR ^a Inject	TTR ^a Contralateral	TTR+HA ^a Inject	TTR+HA ^a Contralateral	TM ^a 1 week	TM ^a 3 weeks
Femur						
Tb.N	0.92 (0.07)	0.80 (0.06) ^b	0.94 (0.12)	0.84 (0.12) ^e	1.13 (0.08)	1.12 (0.02)
Tb.Th (mm)	0.96 (0.04)	0.84 (0.05) ^c	0.90 (0.10)	0.91 (0.09)	1.04 (0.08)	1.03 (0.04)
Tb.Sp (mm)	1.13 (0.09)	1.30 (0.11) ^d	1.09 (0.19)	1.26 (0.21)	0.87 (0.06)	0.87 (0.02)
Tibia						
Tb.N	0.92 (0.10)	0.76 (0.22)	0.89 (0.10)	0.89 (0.18)	1.09 (0.12)	1.15 (0.07)
Tb.Th (mm)	0.98 (0.06)	0.80 (0.18)	1.00 (0.09)	1.00 (0.11)	1.00 (0.04)	1.03 (0.02)
Tb.Sp (mm)	1.10 (0.14)	1.03 (0.19)	1.13 (0.17)	1.16 (0.30)	0.91 (0.11)	0.86 (0.07)

^aData are expressed relative to UI (for TTR ± HA) or Cage (for TM) age matched controls. Injected and Contralateral legs were analyzed separately for the TTR or TTR+HA groups. ^{b-d}Statistical significance was calculated using 1-way ANOVA software and number of animals analyzed for each group is given in [Table S1](#). P=^b0.0045; ^c0.015; ^d0.0059; ^e0.042.

Table 2. Changes in epiphyseal trabecular bone properties following TTR, TTR+HA and TM treatments

Parameter	TTR ^a Inject	TTR ^a Contralateral	TTR+HA ^a Inject	TTR+HA ^a Contralateral	TM ^a 1 week	TM ^a 3 weeks
Femur						
Tb.N	1.01 (0.01)	0.97 (0.03)	0.94 (0.12)	0.96 (0.02)	1.02 (0.03)	1.03 (0.05)
Tb.Th (mm)	0.91 (0.02)	0.89 (0.04) ^b	0.90 (0.10)	0.95 (0.06)	0.98 (0.04)	1.08 (0.11)
Tb.Sp (mm)	1.06 (0.07)	1.09 (0.05)	1.09 (0.19)	1.06 (0.06)	1.04 (0.01)	0.95 (0.05)
Tibia						
Tb.N	1.01 (0.04)	0.92 (0.07)	0.89 (0.10)	1.05 (0.05)	0.89 (0.09)	0.92 (0.09)
Tb.Th (mm)	0.96 (0.07)	1.04 (0.06)	1.00 (0.09)	0.96 (0.07)	1.18 (0.24)	1.18 (0.11)
Tb.Sp (mm)	0.89 (0.05)	0.97 (0.05)	1.13 (0.17)	0.98 (0.05)	1.11 (0.18)	1.04 (0.13)

^aData are expressed relative to UI (for TTR ± HA) or Cage (for TM) age matched controls, as mean (± SD) Injected and Contralateral legs were analyzed separately for the TTR or TTR+HA groups. ^bStatistical significance was calculated using 1-way ANOVA software and number of animals analyzed for each group is given in [Table S1](#). P=^b0.043.

ment groups sacrificed on days 19 and 26. BV/TV, Tb.N, Tb.Th and Tb.Sp were quantitated for the epiphyseal and metaphyseal regions of the femur and the tibia ([Figure S3](#)). Because essentially identical data was obtained at the two time points, it was combined for statistical comparisons ([Figure 4](#) and [Tables 1, 2](#)).

Relative to un-injured controls, the TTR model had no effect on any femoral or tibial bone parameters in the injected leg. However, it resulted in marked changes in the femurs of the contralateral leg. Thus, statistically significant reductions (25-40%) in bone parameters (BV/TV, Tb.N, Tb.Th and Tb.Sp) were detected in the metaphyseal regions of the contralateral femur ([Table 1](#)). In addition, minor reductions in trabecular spacing in the femoral epiphyses of the contralateral leg (P=0.044) and the BV/TV of the femoral cortical bone of the injected leg were observed ([Figure S4](#)).

HA injections had no detectable effect on bone in the injected legs. HA injections also did not alter the marked reductions in all measured parameters in the metaphyseal regions of the femur in the contralateral legs.

Effect of treadmill running without TGFβ1 injection

The decrease in contralateral metaphyseal bone parameters in the TTR model ([Figure 4](#) and [Table 1](#)) was not due to treadmill running alone, but required TGFβ1 injection before treadmill activity. However, the BV/TV of the femoral metaphyses was increased by treadmill alone at 1 and 3 weeks and that of the tibial metaphysis at 3 weeks. Since no detectable changes in trabecular parameters relative to age-matched naïve controls were detected, the TM-induced increase in BV/TV was due to cortical bone in the metaphysis.

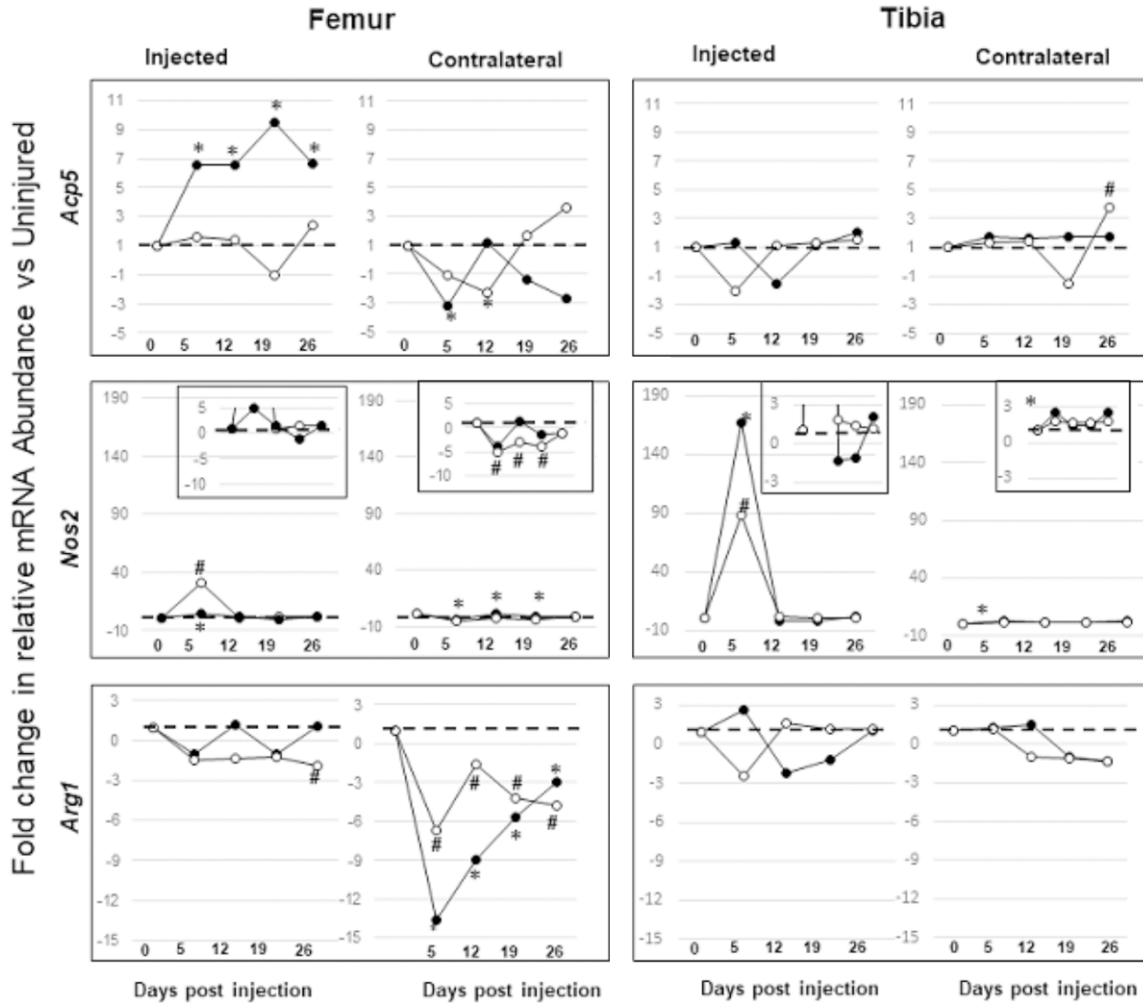


Figure 5. Effect of TTR (●) and TTR+HA (○) on fold changes (vs naïve) in expression of *Acp5*, *Nos2* and *Arg1* in the femoral epiphyses of the injected and contralateral legs. (—) indicates unchanged expression. (*) and (#) indicate $P < 0.05$ for TTR and TTR+HA, respectively, as determined by 1 way ANOVA test of data from $n = 3$ biological replicates. Insets show data on expanded scales.

Osteolytic bone changes in the contralateral leg of the TTR model and the effect of HA treatment on expression of bone-related genes

The lack of effect of HA treatment on bone structure was unexpected, since it had marked effects on inflammatory responses in both femoral epiphyses (which includes the growth plate and metaphyseal calcified cartilage regions) via the *Nfkb* pathway (Figures 2 and 3). We therefore extended our study to examine how expression of genes related to inflammation-mediated bone osteolysis such as osteoclastic *Acp5* [28, 29], M1-macrophagic *Nos 2* [30-32] and M2-macrophagic *Arg1* [33, 34] might be affected by the TTR alone and/or with therapeutic HA. The fold changes in expression of these three genes, in injected and contralateral femo-

ral and tibial specimens are summarized in **Figure 5**.

In the femoral samples of the injected leg of the TTR model (no detectable bone loss), the transcript levels for *Acp5* and *Nos2* were significantly elevated at the acute stage (d5) and *Acp5* remained above uninjured levels (~7-10 fold) up to 26 days. HA therapy abolished the increase in *Acp5*, but not *Nos2*, and whereas *Arg1* expression was not significantly altered due to the TTR model alone, a ~2 fold decrease ($P < 0.05$) was detected on days 12 and 26 following HA therapy.

By comparison, in the femoral samples of the contralateral leg (significant trabecular bone loss), a robust decrease in transcript abun-

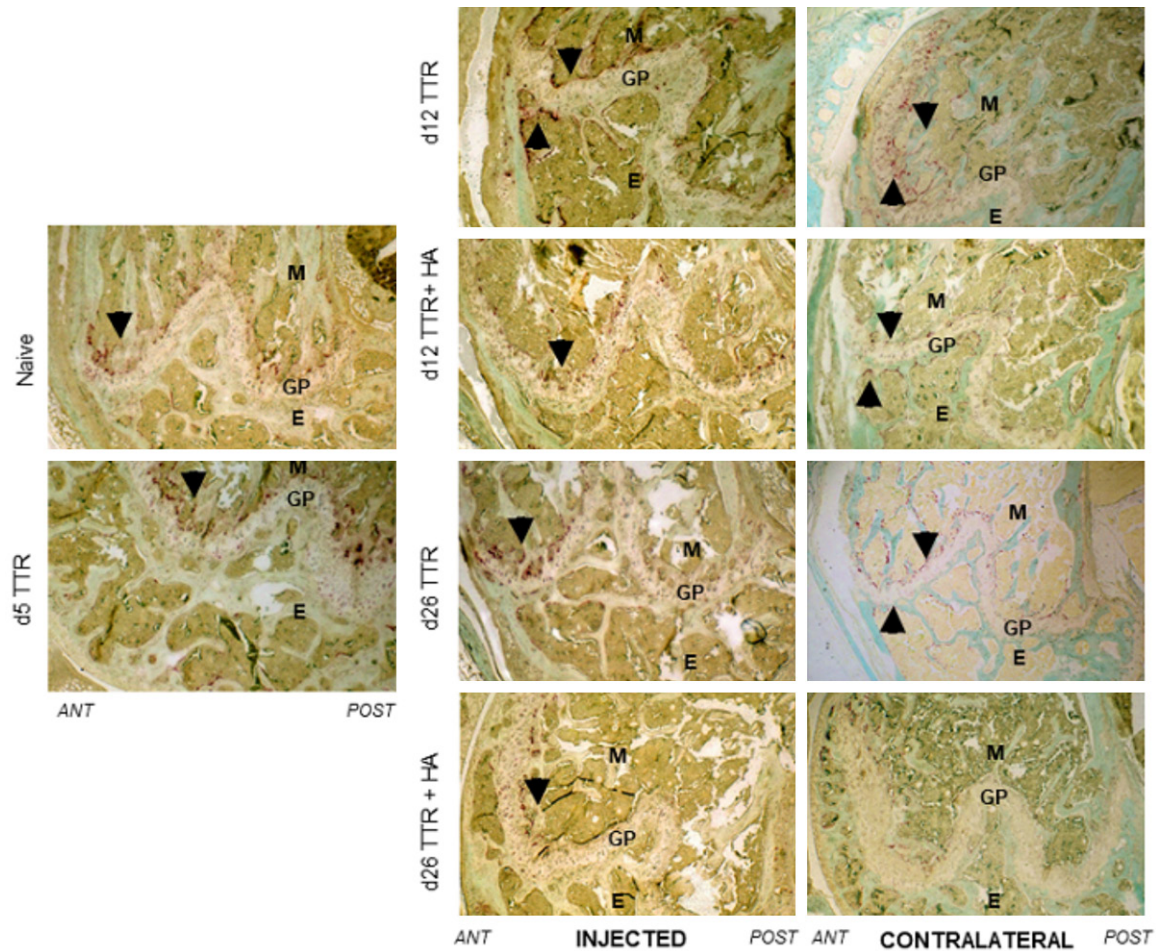


Figure 6. TRAP activity in the femoral epiphyseal and metaphyseal growth plate regions from injected and contralateral joints. 5 μ m thin sections were stained for TRAP product using a SIGMA kit and counterstained with Fast-Green (see Methods). Regions containing TRAP-positive cells are indicated by black arrow heads. In naïve joints, these were abundant on epiphyseal and particularly metaphyseal aspects of the growth plate, but become less abundant in all injected joints by 26 days, with isolated active cell groups on the metaphyseal aspect only. ANT = Anterior, POST = Posterior; M = Metaphysis; E = Epiphyses; GP = Growth Plate.

dance for all 3 genes *Acp5*, *Nos2*, *Arg1* was seen in the acute phase (d5), and this was maintained for *Nos2* and *Arg1* for up to 26 d ($P < 0.05$ vs uninjured controls). Following HA therapy the decreases in *Nos2* and *Arg1* expression were sustained (relative to uninjured controls) whereas *Acp5* levels were variable.

In the tibial samples of the injected leg, only *Nos2* transcript abundance was increased in the acute phase (d5), showing increases in the injected leg of ~ 170 and ~ 90 fold for TTR and TTR+HA, respectively. A minor (~ 3 fold) increase ($P < 0.05$) in *Nos2* expression in the contralateral tibia was also noted with TTR. While *Acp5* and *Arg1* showed apparent decreases in tibial expression, none of these changes reached

statistical significance. Further, there was no major effect of TTR or TM alone on the diaphyseal femoral cortical bone (Figure S3), however a minor ($\sim 3\%$), but statistically significant, reduction in the BV/TV of the femoral cortical bone with TTR (\pm HA) was observed. In keeping with the absence of major structural change we did not detect any effect of the treadmill only on expression of bone resorptive marker genes, *Nos2*, *Arg1* or *Acp5* in epiphyseal samples.

Protein levels and enzyme activity of bone resorption markers in the TTR model

The finding that the osteolytic response to TTR of the contralateral femoral compartment was accompanied by a decreased expression of

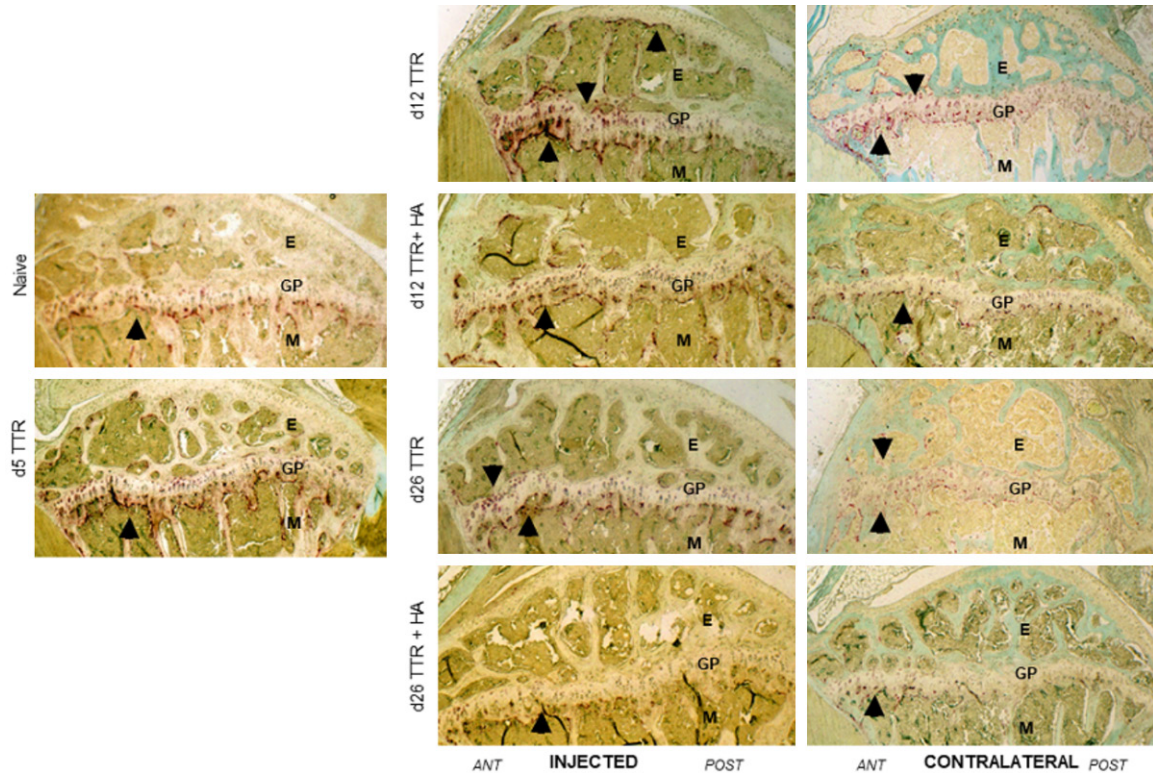


Figure 7. TRAP Staining of the tibial epiphyseal and metaphyseal growth plate regions from Injected and contralateral joints. Regions containing TRAP positive cells are indicated by black arrow heads. In Naïve joints, these are abundant on the metaphyseal aspects of the growth plate, and can also be seen at the anterior aspects of the subchondral bone region. In injected joints, by 26 days, the presence of such cells is greatly diminished. ANT = Anterior, POST = Posterior; M = Metaphysis; E = Epiphyses; GP = Growth Plate.

Acp5 (TRAP), and also *Nos2* and *Arg1* suggested that control of pro- and anti-inflammatory macrophage activity may play a critical role in resorption in this model. To investigate this further, we stained whole joint sections for tartrate-resistant acid phosphatase (TRAP) (Figures 6, 7), *NOS2* (Figures 8, 10) and Arginase 1 (Figures 9, 11). TRAP staining in naive joints was predominantly in the metaphyseal regions (calcified cartilage) of both femoral and tibial growth plates (black arrowheads Figures 6, 7 UI panels) and no major changes were detected in TTR with time after induction. However, HA therapy decreased intensity of the TRAP staining from TTR levels in both injected and contralateral legs, at d12 and d26, but not in the acute phase (d5, data not shown). Notably, the significantly increased transcript abundance of *Acp5* in the femoral compartment of the TGF β 1 injected joints (Figure 4) was not accompanied by an increase in active TRAP in these joints.

NOS2 immunostaining in naive joints (Figures 8, 9) was largely restricted to the perichondrial/periosteal lining in both tibial and femoral compartments. However, with TTR, *NOS2* immunoreactivity increased in both tibial and femoral growth plates (cell-associated and ECM, see high mag insert), as well in regions of the metaphyseal/epiphyseal bone marrow, adjacent to the trabeculae and within the trabeculae. In this case, the increase in protein levels with TTR were entirely in keeping with the increased levels of *Nos2* mRNA transcripts seen at d5 in injected joints (Figure 4). Furthermore, high *NOS2* immunostaining was seen at all times up to d29, suggesting that the protein (or at the least the epitope recognized by the antibody) exhibits a prolonged half-life in the tissues. In the contralateral legs, *NOS2* protein was barely detectable in either the growth plate or bone marrow compartments of the femur and tibia, although there was some increased staining in the trabecular bone itself.

Therapeutic hyaluronan and bone remodeling in osteoarthritis

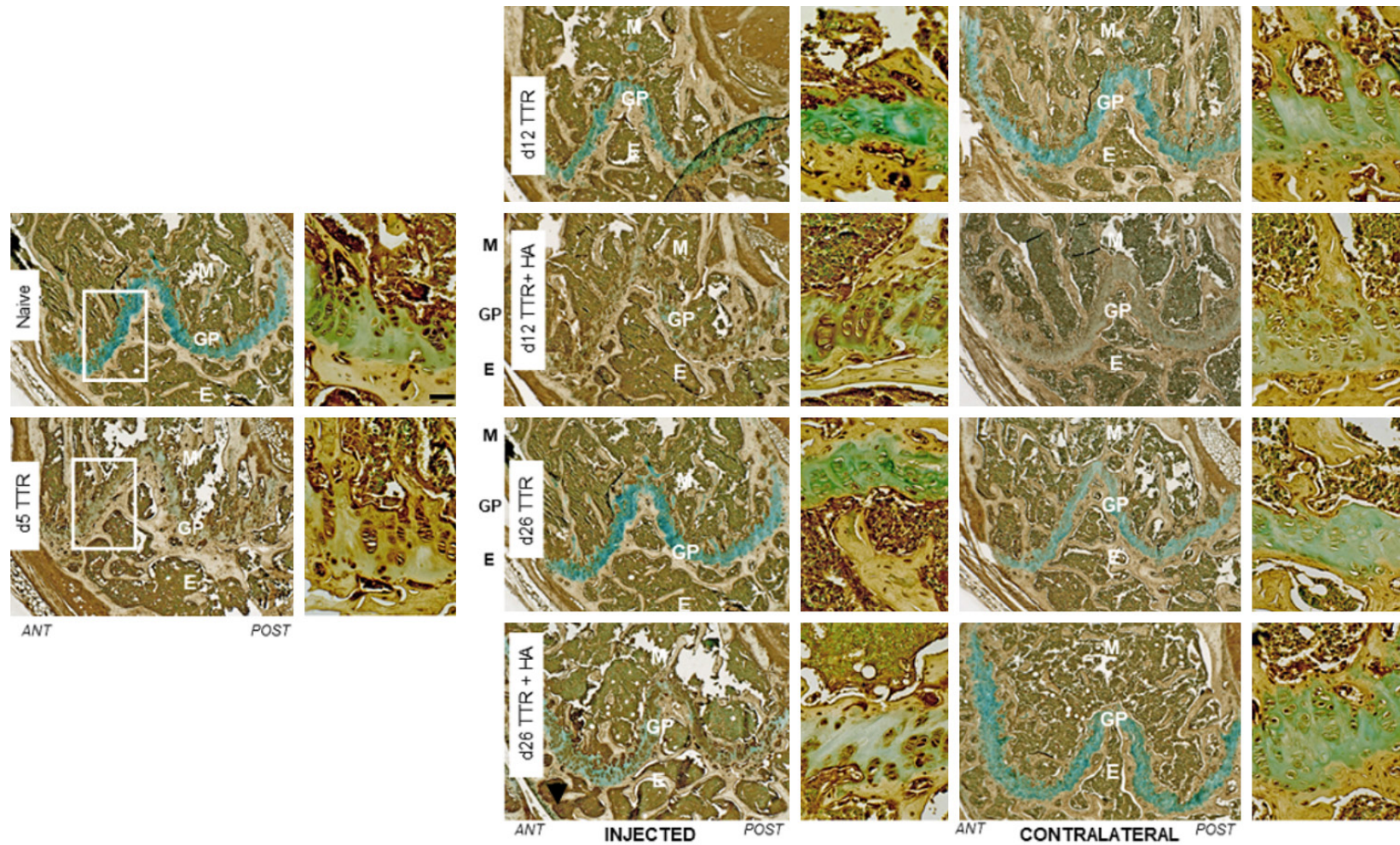


Figure 8. NOS2 IHC staining of the femoral epiphyseal and metaphyseal growth plate regions from injected and contralateral joints. Right hand panels in each column show a higher magnification of the growth plate and adjacent epiphyseal and metaphyseal regions. ANT = Anterior, POST = Posterior; M = Metaphysis; E = Epiphyses; GP = Growth Plate. (-) = 20 um in high magnification panels. Non-immune control staining is shown in [Figure S5](#).

Therapeutic hyaluronan and bone remodeling in osteoarthritis

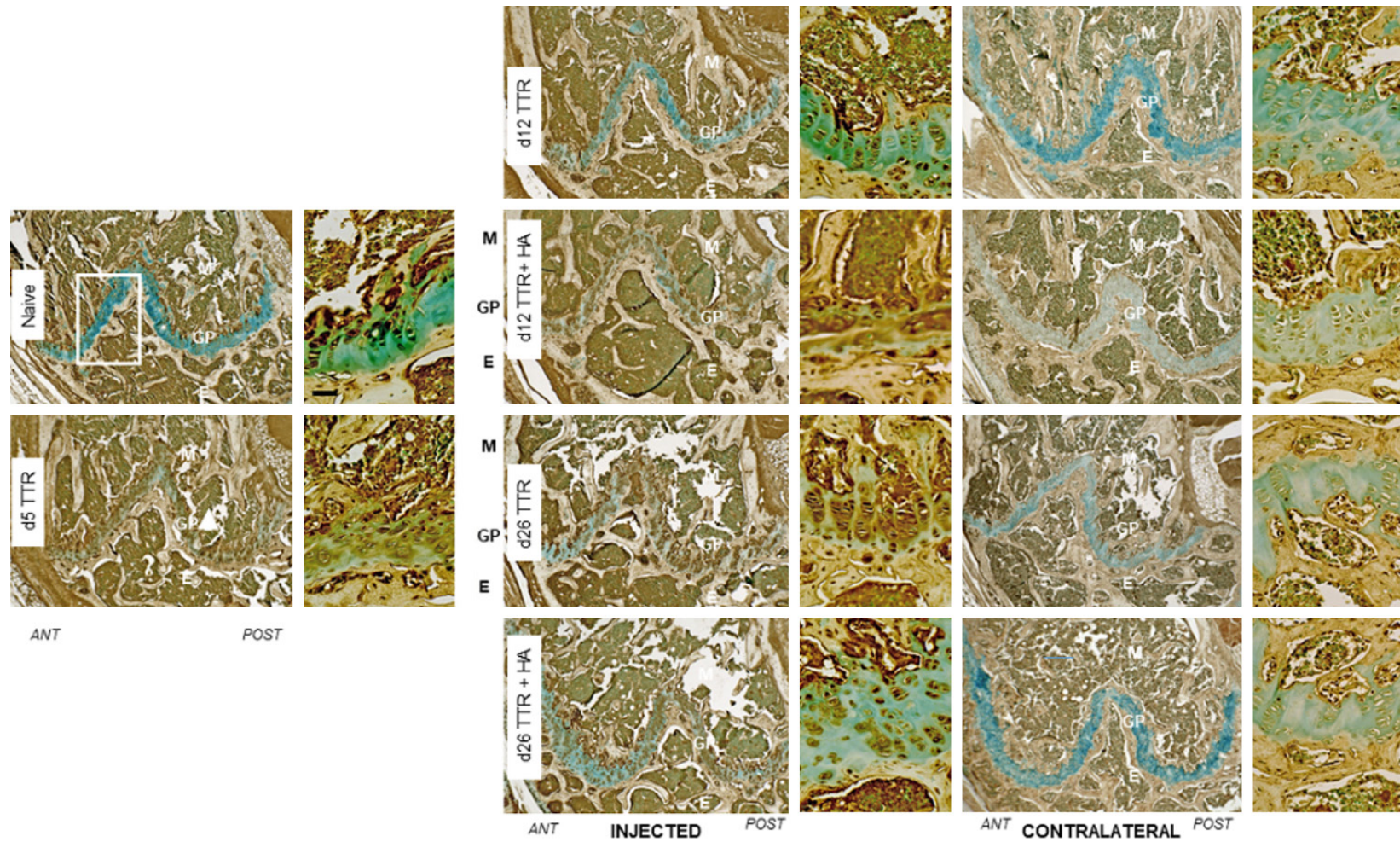


Figure 9. Arginase 1 IHC staining of the femoral epiphyseal and metaphyseal growth plate regions from injected and contralateral joints. Right hand panels in each column show a higher magnification of the growth plate and adjacent epiphyseal and metaphyseal regions. ANT = Anterior, POST = Posterior; M = Metaphysis; E = Epiphyses; GP = Growth Plate. (-) = 20 um in high magnification panels. Non-immune control staining is shown in [Figure S5](#).

Therapeutic hyaluronan and bone remodeling in osteoarthritis

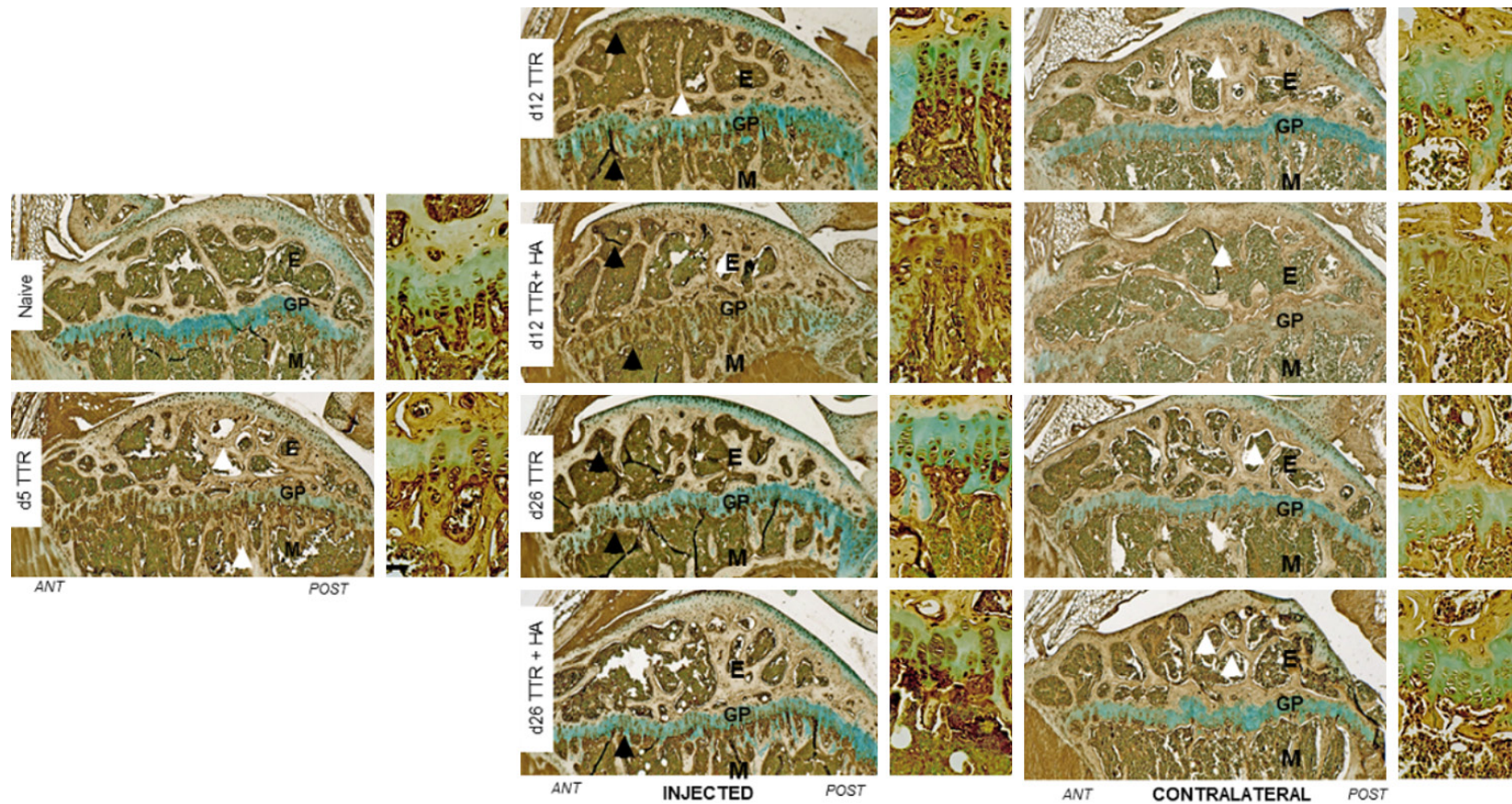


Figure 10. NOS2 IHC staining of the tibial epiphyseal and metaphyseal growth plate regions from injected and contralateral joints. Right hand panels in each column show a higher magnification of the growth plate and adjacent epiphyseal and metaphyseal regions. ANT = Anterior, POST = Posterior; M = Metaphysis; E = Epiphyses; GP = Growth Plate. (-) = 20 um in high magnification panels. Non-immune control staining is shown in [Figure S5](#).

Therapeutic hyaluronan and bone remodeling in osteoarthritis

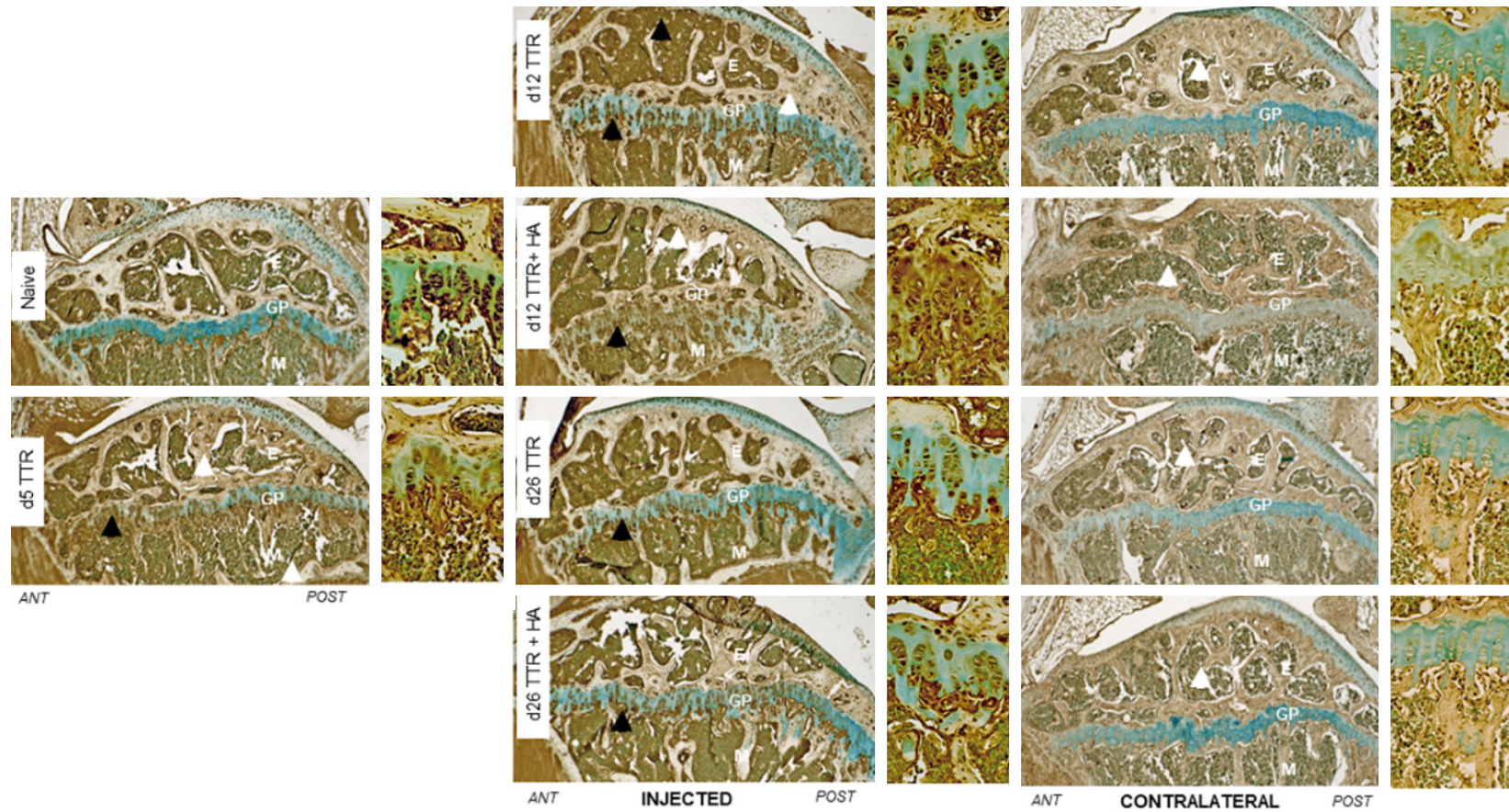


Figure 11. Arginase 1 IHC staining of the tibial epiphyseal and metaphyseal growth plate regions from injected and contralateral joints. Right hand panels in each column show a higher magnification of the growth plate and adjacent epiphyseal and metaphyseal regions. ANT = Anterior, POST = Posterior; M = Metaphysis; E = Epiphyses; GP = Growth Plate. (-) = 20 um in high magnification panels. Non-immune control staining is shown in [Figure S5](#).

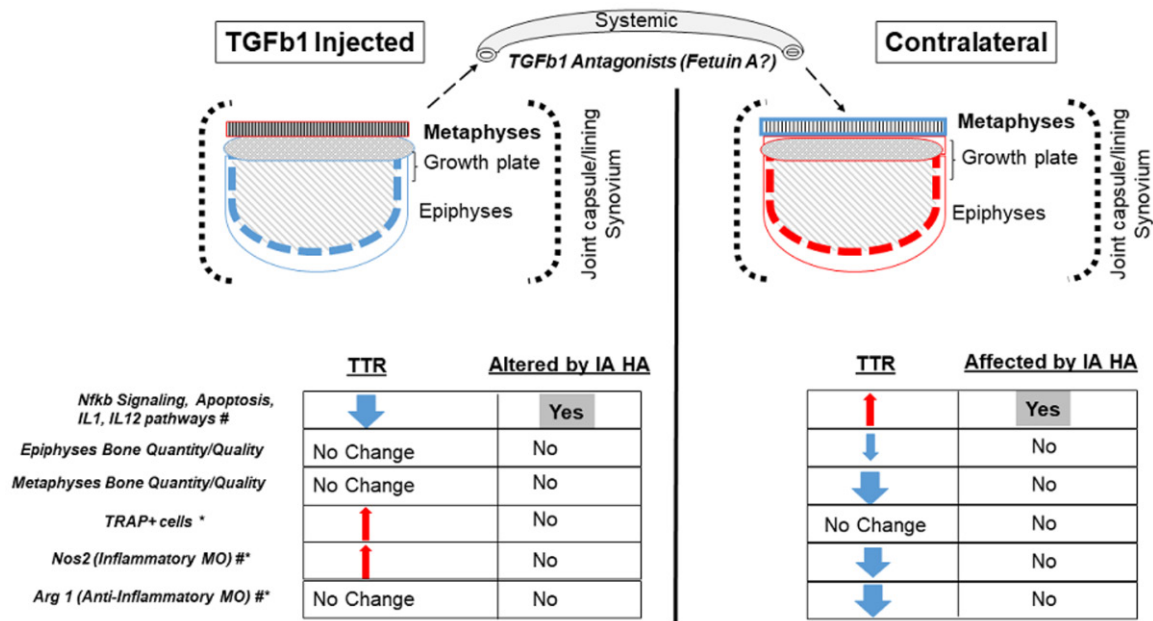


Figure 12. Schema illustrating the alterations in inflammatory pathway genes and bone remodeling in the femoral epiphyses and metaphyses of the TTR OA model and after of IA HA. Femoral compartments (epiphyses/growth plate/metaphyses), lined by joint capsule and synovial tissue (---) from both, TGFb1-Injected and Contralateral legs are shown. All three compartments were combined for gene expression and histological analyses (see Methods), whereas epiphyseal and metaphyseal trabecular bone parameters were quantitated separately. Increases or decreases in gene expression, bone structure or macrophage (MO)-like cell types in injected vs contralateral knees are shown in red or blue arrows and outlines, respectively. (AC = Articular Cartilage, #Gene expression; *Protein IHC).

Again, this low abundance is entirely consistent with the expression data obtained (Figure 4).

Arginase 1 staining in naïve joints was restricted to the metaphyseal regions of both femoral and tibial growth plates, and thus was similar in distribution to NOS2 protein (Figure 6 vs Figure 7; Figure 9 vs Figure 1). Following TTR induction, a robust increase in staining was detected in the growth plate regions, with strongest staining in the hypertrophic and calcified cartilage zones for both femur and tibia (Figures 7 and 10). Whereas the TTR-induced increases in NOS2 protein decreased significantly at d12 and further at d26, Arginase 1 protein remained increased throughout the experimental period. This, together with the lack of significant changes in expression in either femur or tibia suggests a possibly important role for post-translational control of Arginase 1 protein turnover in these locations.

In contralateral joints, at all experimental time points, Arginase 1 protein was barely detectable in the femoral and tibial epiphysis and metaphysis, and growth plate region. Notably,

whereas TTR did not affect *Arg1* gene expression in either femur or tibia of the injected legs, in the contralateral femur they were strongly inhibited (~15 fold) at the acute post-injection stage (d5) and remained significantly lower than naïve levels throughout the experimental period. Thus, it appears that a combination of suppressed levels of *Arg1* mRNA in combination with lack of Arginase 1 protein bring about the increased trabecular osteolysis seen in the metaphyseal and epiphyseal compartments of the contralateral femur. This suggests that a lack of protective Arginase-1 positive M2 macrophages leaves the associated bone vulnerable to osteolysis.

In keeping with the lack of effect of therapeutic HA on the bone remodeling in either the injected or contralateral legs (Table 1), HA also did not influence the abundance of NOS2 or Arginase proteins, nor did it markedly modify their expression under any experimental condition or in any tissue compartment (Figure 4, open circles, Figures 6, 7, 9, 10). However, since therapeutic HA strongly modified the expression levels of a large number of genes

in the Nfkb pathway in the same tissue compartments (epiphyses, growth-plate and calcified cartilage), the inflammatory signaling pathways resulting in the trabecular bone resorption of the contralateral leg seen in this model, are probably not primarily Nfkb-related but Arginase 1-related.

Discussion

When considered as a whole, the gene expression changes in the TTR model illustrate that for Nfkb signaling genes, the response to unilateral TTR injury was very disparate in the two knees and also in the two knee compartments (**Figure 12**). The time-course profile was very typical of a phasic biological response in which the initial effector (in this case TGF β 1) generates short-term change and is predictably lost from the system by diffusion (change is normalized) to be replaced by a second effector with a long-term effect. Since many of the genes exhibited inhibition in both phases (and the extent of inhibition was similar in each) the result is consistent with the first phase resulting from the exogenous TGF β 1 and the second phase being due to endogenous TGF β 1, perhaps a product of resident tissue macrophages.

The disparate set of responses illustrates the capacity for the expression of Nfkb pathway genes to be affected by both local environmental differences (cell populations, biomechanics) and also by systemic effects (circulating factors and hormonal responses). Indeed only 3/74 genes (*Ccl2*, *Bcl3*, *Nfkb1a*) could be considered as generalized markers in that they showed the same response, an inhibition, in all locations at one or more times. The finding that 21 genes (*Cd27*, *Csf2*, *Egfr*, *Lta*, *Tnfsf10*, *Ikbkb*, *Ikbke*, *Ikbkg*, *Nfkb1*, *Casp1*, *Casp8*, *Cflar*, *Irf1*, *Csf3*, *Csf1*, *Akt1*, *Eif2ak2*, *Atf1*, *Atf2*, *Crebbp*, *Smad3*) were inhibited in the injected femur but activated contemporaneously (day 5) in the contralateral femur, suggests that the contralateral changes were not due to circulation of exogenous TGF β 1, but rather a release into the circulation from the injected joint of counteracting factor(s) with the capacity to activate (rather than inhibit) expression of the 21 genes. This interpretation is also supported by the delay to day 12 of the first activation of 16 genes in the contralateral tibia.

The functional (GO term) group analysis (Genemania, University of Toronto) of this 21-gene group, on the biological basis selection, generated the following descending hierarchy of affected processes: (positive regulation of cytokine production; positive regulation of leukocyte differentiation; extrinsic apoptotic signaling pathway; regulation of interleukin-12 biosynthetic process; I-kappaB kinase/NF-kappa signaling; regulation of cysteine-type endopeptidase activity; myeloid cell differentiation; lymphocyte apoptotic process; regulation of leukocyte differentiation; transcription regulatory region sequence-specific DNA binding; myeloid leukocyte differentiation). The strong emphasis on cell differentiation processes in this listing suggests that a major early effect of the TTR model is to suppress myeloid differentiation in the femur of the injected joint, but to promote this process in the contralateral femur. This is consistent with the starkly different effects on femoral bone structure in the two limbs.

To further delineate the IA HA effect, we also performed the functional (GO term) group analysis (Genemania, University of Toronto) of the 25 genes phasically affected by HA (on the *biological basis* selection). This revealed that HA primarily affected Nfkb regulated apoptotic responses at the site of action in the injected limb. In addition to its apparent effects on apoptosis in the injected limb, HA injection phasically modified pro-inflammatory Nfkb signaling events, particularly those involving IL-1 and IL-12 in the same limb (**Figure 12**).

Unlike for the TGF β 1 effects, injection of HA did not result in extensive tibial or contralateral changes in expression levels. This is despite the fact that injection of HA on day 4 appeared to normalize the deficiencies in Tb.N in the femoral sub-chondral bone of the contralateral leg, whereas it had no detectable effect on the low BV/TV in the contralateral metaphysis (**Figure 12**).

The finding of bone resorption in the contralateral leg in the TTR model appears to distinguish it from other models of OA [35, 36], although contralateral effects have not been commonly studied. Notably, the osteolytic response of the contralateral epiphyses is induced only after injection of TGF β 1, as the treadmill run controls show increased bone mass, which is consistent

Therapeutic hyaluronan and bone remodeling in osteoarthritis

with the previously published bone anabolism following treadmill running [37, 38].

Therefore, we speculate that the remodeling effect in the contralateral limb is likely due to the high concentration of TGF β 1 injected into the other knee. Thus a suppression of TGF β 1 action at sites remote from the initial injury would be expected to provide a protective effect against ectopic bone formation, and therefore in the present model a re-activation of growth plate calcification and bone deposition in the contralateral limb. Indeed, Fetuin A could be a potential candidate for such a protective action against excessive TGF β 1 action, as has been reported for a number of tissues and organs, including bone [39-41].

Based on both gene expression and IHC analyses, the osteolytic activity in the femoral metaphysis (and partly epiphyses) of the contralateral leg of the TTR model (with or without HA injection) appears to be linked to the suppression of Arg1 gene expression and absence of Arginase 1 protein [42, 43] in cells at this site.

It is suggested that the lack of action of anti-inflammatory macrophage activity [44] as indicated by decreased transcript and protein abundance of Arginase 1 [29], could cause increases in NO production via NOS2 [42] and thus continued bone resorption via M2 (inflammatory) macrophage-type cells [32, 33, 45] rather than mature TRAP-positive osteoclasts). Indeed the role of fibroblasts and macrophages in osteolysis have been well described at sites of bone loss associated with aseptic or particle induced implant loosening [46-50]. This, together with the finding that IA TGF β 1 alone or in combination with HA also results in depression of bone-cell specific genes such as *Bglap* (osteocalcin) and *Tnfsf11* (RANKL) (Figures S6 and S7) is consistent with it mediating an overall disruption of the trabecular structure in the femoral compartment of contralateral legs.

Regarding injected legs, the finding that the TGF β 1 and HA effects were primarily in the femoral compartment might be related to the previous finding that injected HA primarily localizes to this compartment [10], and is also rapidly cleared from there. Indeed a more recent study employing IA injection of both single chain and crosslinked HA [51] confirmed the distribution

of the injected HA primarily to the femora-patella compartment. Thus injected TGF β 1 may similarly distribute and predominantly affect cells at those tissue sites. Whether IA HA modifies the TGF β 1 mediated changes in Nfkb signaling genes via direct effects on the TGF β /RII complex or indirectly via signaling through one of more of its receptors (CD44, TLR2, TLR4) remains to be established. Similarly, whether such regulatory action occur on the same cell is mediated by a paracrine response between different cells types in the joint requires further investigation. In addition, since bone resorption in the contralateral leg is also restricted to the femoral compartment, the data supports the idea that mechanical inputs from treadmill running modulate cell responses in tibial and femora-patellar compartments differently [20, 38].

In conclusion, the finding that IA causes a temporary inhibition of Nfkb-pathway gene expression in the femoral epiphyses/metaphyses, but has no effect on structural bone parameters in that compartment, might be related to the dwell-time of HA, which in this study was restricted to a single dosage, whereas in clinical practice therapeutic HA is currently dosed multiple times. Thus such multiple dosages of crosslinked products might exert a more long lasting effect on the soft tissues in the joint itself [51-53] and thus influence systemic regulators of macrophage-controlled inflammation at distant sites. Moreover, OA models, which display subchondral bone remodeling should also be employed in the future to elucidate potential therapeutic effects of intra-articular HA on bone metabolism.

Acknowledgements

Funding was provided by Seikagaku Corporation (AP), Arthritis Foundation (DC) and the Katz Rubschlager Endowment for OA Research (AP). AP, RR, QS, JL, DC have no conflicts of interest to declare, JT is an employee of Seikagaku Corporation Inc.

Disclosure of conflict of interest

None.

Abbreviations

DMM, Destabilized Medial Meniscus; HA, Hyaluronan; IA, Intra-Articular; IHC, Immuno-

histochemistry; micro CT, micro Computed Tomography; OA, Osteoarthritis; TGFβ1, Transforming Growth Factor beta 1; TRAP, Tartrate Resistant Alkaline Phosphatase; TTR, TGFβ1 injection with Treadmill Running.

Address correspondence to: Dr. Anna Plaas, Department of Internal Medicine (Rheumatology), Rush University Medical Center, Chicago, IL, USA. E-mail: aplaas@gmail.com; anna_plaas@rush.edu

References

- [1] Maheu E, Bannuru RR, Herrero-Beaumont G, Allali F, Bard H and Migliore A. Why we should definitely include intra-articular hyaluronic acid as a therapeutic option in the management of knee osteoarthritis: results of an extensive critical literature review. *Semin Arthritis Rheum* 2018; [Epub ahead of print].
- [2] Akman YE, Sukur E, Senel A, Oztas Sukur NE, Talu CK and Ozturkmen Y. The comparison of the effects of a novel hydrogel compound and traditional hyaluronate following micro-fracture procedure in a rat full-thickness chondral defect model. *Acta Orthop Traumatol Turc* 2017; 51: 331-336.
- [3] Kaderli S, Viguier E, Watrelot-Virieux D, Roger T, Gurny R, Scapozza L, Moller M, Boulocher C and Jordan O. Efficacy study of two novel hyaluronic acid-based formulations for viscosupplementation therapy in an early osteoarthrosic rabbit model. *Eur J Pharm Biopharm* 2015; 96: 388-395.
- [4] Fosco M and Dagher E. Proposal of a therapeutic protocol for selected patients with patellofemoral knee osteoarthritis: arthroscopic lateral retinacular release followed by viscosupplementation. *Musculoskelet Surg* 2016; 100: 171-178.
- [5] Frisbie DD, McIlwraith CW, Kawcak CE and Werpy NM. Evaluation of intra-articular hyaluronan, sodium chondroitin sulfate and N-acetyl-D-glucosamine combination versus saline (0.9% NaCl) for osteoarthritis using an equine model. *Vet J* 2013; 197: 824-829.
- [6] Strauss E, Schachter A, Frenkel S and Rosen J. The efficacy of intra-articular hyaluronan injection after the microfracture technique for the treatment of articular cartilage lesions. *Am J Sports Med* 2009; 37: 720-726.
- [7] Gunes T, Bostan B, Erdem M, Koseoglu RD, Asci M and Sen C. Intraarticular hyaluronic acid injection after microfracture technique for the management of full-thickness cartilage defects does not improve the quality of repair tissue. *Cartilage* 2012; 3: 20-26.
- [8] Tuncay I, Erkokcak OF, Acar MA and Toy H. The effect of hyaluronan combined with microfracture on the treatment of chondral defects: an experimental study in a rabbit model. *Eur J Orthop Surg Traumatol* 2013; 23: 753-758.
- [9] Plaas A, Li J, Riesco J, Das R, Sandy JD and Harrison A. Intraarticular injection of hyaluronan prevents cartilage erosion, periarticular fibrosis and mechanical allodynia and normalizes stance time in murine knee osteoarthritis. *Arthritis Res Ther* 2011; 13: R46.
- [10] Muramatsu Y, Sasho T, Saito M, Yamaguchi S, Akagi R, Mukoyama S, Akatsu Y, Katsuragi J, Fukawa T, Endo J, Hoshi H, Yamamoto Y and Takahashi K. Preventive effects of hyaluronan from deterioration of gait parameters in surgically induced mice osteoarthritic knee model. *Osteoarthritis Cartilage* 2014; 22: 831-835.
- [11] Li J, Gorski DJ, Anemaet W, Velasco J, Takeuchi J, Sandy JD and Plaas A. Hyaluronan injection in murine osteoarthritis prevents TGFbeta 1-induced synovial neovascularization and fibrosis and maintains articular cartilage integrity by a CD44-dependent mechanism. *Arthritis Res Ther* 2012; 14: R151.
- [12] Chen WH, Lo WC, Hsu WC, Wei HJ, Liu HY, Lee CH, Tina Chen SY, Shieh YH, Williams DF and Deng WP. Synergistic anabolic actions of hyaluronic acid and platelet-rich plasma on cartilage regeneration in osteoarthritis therapy. *Biomaterials* 2014; 35: 9599-9607.
- [13] Zhang Z, Wei X, Gao J, Zhao Y, Zhao Y, Guo L, Chen C, Duan Z, Li P and Wei L. Intra-articular injection of cross-linked hyaluronic acid-dexamethasone hydrogel attenuates osteoarthritis: an experimental study in a rat model of osteoarthritis. *Int J Mol Sci* 2016; 17: 411.
- [14] Duan X, Sandell LJ, Chinzei N, Holguin N, Silva MJ, Schiavinato A and Rai MF. Therapeutic efficacy of intra-articular hyaluronan derivative and platelet-rich plasma in mice following axial tibial loading. *PLoS One* 2017; 12: e0175682.
- [15] Piuze NS, Midura RJ, Muschler GF and Hascall VC. Intra-articular hyaluronan injections for the treatment of osteoarthritis: perspective for the mechanism of action. *Ther Adv Musculoskelet Dis* 2018; 10: 55-57.
- [16] Avenoso A, D'Ascola A, Scuruchi M, Mandraffino G, Calatroni A, Saitta A, Campo S and Campo GM. Hyaluronan in experimental injured/inflamed cartilage: in vivo studies. *Life Sci* 2018; 193: 132-140.
- [17] Weber A, Chan PMB and Wen C. Do immune cells lead the way in subchondral bone disturbance in osteoarthritis? *Prog Biophys Mol Biol* 2017; [Epub ahead of print].
- [18] Coughlin TR and Kennedy OD. The role of subchondral bone damage in post-traumatic osteoarthritis. *Ann N Y Acad Sci* 2016; 1383: 58-66.

Therapeutic hyaluronan and bone remodeling in osteoarthritis

- [19] Findlay DM and Kuliwaba JS. Bone-cartilage crosstalk: a conversation for understanding osteoarthritis. *Bone Res* 2016; 4: 16028.
- [20] Jia H, Ma X, Wei Y, Tong W, Tower RJ, Chandra A, Wang L, Sun Z, Yang Z, Badar F, Zhang K, Tseng WJ, Kramer I, Kneissel M, Xia Y, Liu XS, Wang JH, Han L, Enomoto-Iwamoto M and Qin L. Loading-induced reduction in sclerostin as a mechanism of subchondral bone plate sclerosis in mouse knee joints during late-stage osteoarthritis. *Arthritis Rheumatol* 2018; 70: 230-241.
- [21] Alliston T, Hernandez CJ, Findlay DM, Felson DT and Kennedy OD. Bone marrow lesions in osteoarthritis: what lies beneath. *J Orthop Res* 2018; 36: 1818-1825.
- [22] Fennen M, Pap T and Dankbar B. Smad-dependent mechanisms of inflammatory bone destruction. *Arthritis Res Ther* 2016; 18: 279.
- [23] Kanaan RA and Kanaan LA. Transforming growth factor beta1, bone connection. *Med Sci Monit* 2006; 12: RA164-169.
- [24] Matsumoto T and Abe M. TGF-beta-related mechanisms of bone destruction in multiple myeloma. *Bone* 2011; 48: 129-134.
- [25] Blaney Davidson EN, van Caam AP, Vitters EL, Bennink MB, Thijssen E, van den Berg WB, Koenders MI, van Lent PL, van de Loo FA and van der Kraan PM. TGF-beta is a potent inducer of Nerve Growth Factor in articular cartilage via the ALK5-Smad2/3 pathway. Potential role in OA related pain? *Osteoarthritis Cartilage* 2015; 23: 478-486.
- [26] van Beuningen HM, van der Kraan PM, Arntz OJ and van den Berg WB. Transforming growth factor-beta 1 stimulates articular chondrocyte proteoglycan synthesis and induces osteophyte formation in the murine knee joint. *Lab Invest* 1994; 71: 279-290.
- [27] van den Berg WB, van Osch GJ, van der Kraan PM and van Beuningen HM. Cartilage destruction and osteophytes in instability-induced murine osteoarthritis: role of TGF beta in osteophyte formation? *Agents Actions* 1993; 40: 215-219.
- [28] Kubatzky KF, Uhle F and Eigenbrod T. From macrophage to osteoclast - How metabolism determines function and activity. *Cytokine* 2018; 112: 102-115.
- [29] Gu Q, Yang H and Shi Q. Macrophages and bone inflammation. *J Orthop Translat* 2017; 10: 86-93.
- [30] Naidu VG, Dinesh Babu KR, Thwin MM, Satish RL, Kumar PV and Gopalakrishnakone P. RANKL targeted peptides inhibit osteoclastogenesis and attenuate adjuvant induced arthritis by inhibiting NF-kappaB activation and down regulating inflammatory cytokines. *Chem Biol Interact* 2013; 203: 467-479.
- [31] Fukada SY, Silva TA, Saconato IF, Garlet GP, Avila-Campos MJ, Silva JS and Cunha FQ. iNOS-derived nitric oxide modulates infection-stimulated bone loss. *J Dent Res* 2008; 87: 1155-1159.
- [32] Silva MJ, Sousa LM, Lara VP, Cardoso FP, Junior GM, Totola AH, Caliani MV, Romero OB, Silva GA, Ribeiro-Sobrinho AP and Vieira LQ. The role of iNOS and PHOX in periapical bone resorption. *J Dent Res* 2011; 90: 495-500.
- [33] Bhatta A, Sangani R, Kolhe R, Toque HA, Cain M, Wong A, Howie N, Shinde R, Elsalanty M, Yao L, Chutkan N, Hunter M, Caldwell RB, Isales C, Caldwell RW and Fulzele S. Deregulation of arginase induces bone complications in high-fat/high-sucrose diet diabetic mouse model. *Mol Cell Endocrinol* 2016; 422: 211-220.
- [34] Gong D, Shi W, Yi SJ, Chen H, Groffen J and Heisterkamp N. TGFbeta signaling plays a critical role in promoting alternative macrophage activation. *BMC Immunol* 2012; 13: 31.
- [35] Khorasani MS, Diko S, Hsia AW, Anderson MJ, Genetos DC, Haudenschild DR and Christiansen BA. Effect of alendronate on post-traumatic osteoarthritis induced by anterior cruciate ligament rupture in mice. *Arthritis Res Ther* 2015; 17: 30.
- [36] Fang H, Huang L, Welch I, Norley C, Holdsworth DW, Beier F and Cai D. Early changes of articular cartilage and subchondral bone in the DMM mouse model of osteoarthritis. *Sci Rep* 2018; 8: 2855.
- [37] Iwamoto J, Shimamura C, Takeda T, Abe H, Ichimura S, Sato Y and Toyama Y. Effects of treadmill exercise on bone mass, bone metabolism, and calciotropic hormones in young growing rats. *J Bone Miner Metab* 2004; 22: 26-31.
- [38] Li X, Yang J, Liu D, Li J, Niu K, Feng S, Yokota H and Zhang P. Knee loading inhibits osteoclast lineage in a mouse model of osteoarthritis. *Sci Rep* 2016; 6: 24668.
- [39] Szweras M, Liu D, Partridge EA, Pawling J, Sukhu B, Clokie C, Jahnen-Dechent W, Tenenbaum HC, Swallow CJ, Grynepas MD and Dennis JW. alpha 2-HS glycoprotein/fetuin, a transforming growth factor-beta/bone morphogenetic protein antagonist, regulates postnatal bone growth and remodeling. *J Biol Chem* 2002; 277: 19991-19997.
- [40] Harman H, Tekeoglu I, Gurol G, Sag MS, Karakece E, IH CI, Kamanli A and Nas K. Comparison of fetuin-A and transforming growth factor beta 1 levels in patients with spondyloarthropathies and rheumatoid arthritis. *Int J Rheum Dis* 2017; 20: 2020-2027.
- [41] Zhou Y, Yang S and Zhang P. Effect of exogenous fetuin-A on TGF-beta/Smad signaling in

Therapeutic hyaluronan and bone remodeling in osteoarthritis

- hepatic stellate cells. *Biomed Res Int* 2016; 2016: 8462615.
- [42] Wu G, Bazer FW, Davis TA, Kim SW, Li P, Marc Rhoads J, Carey Satterfield M, Smith SB, Spencer TE and Yin Y. Arginine metabolism and nutrition in growth, health and disease. *Amino Acids* 2009; 37: 153-168.
- [43] Villalta SA, Nguyen HX, Deng B, Gotoh T and Tidball JG. Shifts in macrophage phenotypes and macrophage competition for arginine metabolism affect the severity of muscle pathology in muscular dystrophy. *Hum Mol Genet* 2009; 18: 482-496.
- [44] Viniegra A, Goldberg H, Cil C, Fine N, Sheikh Z, Galli M, Freire M, Wang Y, Van Dyke TE, Glogauer M and Sima C. Resolving macrophages counter osteolysis by anabolic actions on bone cells. *J Dent Res* 2018; 97: 1160-1169.
- [45] Yeon JT, Choi SW and Kim SH. Arginase 1 is a negative regulator of osteoclast differentiation. *Amino Acids* 2016; 48: 559-565.
- [46] Purdue PE, Koulouvaris P, Potter HG, Nestor BJ and Sculco TP. The cellular and molecular biology of periprosthetic osteolysis. *Clin Orthop Relat Res* 2007; 454: 251-261.
- [47] Pan X, Mao X, Cheng T, Peng X, Zhang X, Liu Z, Wang Q and Chen Y. Up-regulated expression of MIF by interfacial membrane fibroblasts and macrophages around aseptically loosened implants. *J Surg Res* 2012; 176: 484-489.
- [48] Fujii J, Niida S, Yasunaga Y, Yamasaki A and Ochi M. Wear debris stimulates bone-resorbing factor expression in the fibroblasts and osteoblasts. *Hip Int* 2011; 21: 231-237.
- [49] Ross R, Viridi A, Liu S, Sena K and Sumner D. Particle-induced osteolysis is not accompanied by systemic remodeling but is reflected by systemic bone biomarkers. *J Orthop Res* 2014; 32: 967-73.
- [50] Tamaki Y, Sasaki K, Sasaki A, Takakubo Y, Hasegawa H, Ogino T, Kontinen YT, Salo J and Takagi M. Enhanced osteolytic potential of monocytes/macrophages derived from bone marrow after particle stimulation. *J Biomed Mater Res B Appl Biomater* 2008; 84: 191-204.
- [51] Maudens P, Meyer S, Seemayer CA, Jordan O and Allemann E. Self-assembled thermoresponsive nanostructures of hyaluronic acid conjugates for osteoarthritis therapy. *Nanoscale* 2018; 10: 1845-1854.
- [52] Pradal J, Maudens P, Gabay C, Seemayer CA, Jordan O and Allemann E. Effect of particle size on the biodistribution of nano- and microparticles following intra-articular injection in mice. *Int J Pharm* 2016; 498: 119-129.
- [53] Maudens P, Jordan O and Allemann E. Recent advances in intra-articular drug delivery systems for osteoarthritis therapy. *Drug Discov Today* 2018; 23: 1761-1775.

Therapeutic hyaluronan and bone remodeling in osteoarthritis

Table S1. Experimental groups of mice and biological replicates used for outcome assays

Treatments	Sample ID	QPCR ^a	Histology	Micro CT ^b
Uninjured	UI	N=3 (3,1,1) ^b	N=3	N=4
TTR	5 d	N=3 (3,1,1)	N=3	N=4
	12 d	N=3 (3,1,1)	N=3	N=4
	19 d	N=3 (3,1,1)	ND	N=4
	25 d	N=3 (3,1,1)	N=3	N=4
TTR+HA	5 d	N=3 (3,1,1)	N=3	N=4
	12 d	N=3 (3,1,1)	N=3	N=4
	19 d	N=3 (3,1,1)	ND	N=4
	25 d	N=3 (3,1,1)	N=3	N=4
Cage	19 d	ND	ND	N=4
TM	7 d	ND	ND	N=4
	19 d	ND	ND	N=4

^aFemoral and Tibial Compartments were assayed separately; ^bIndicates the number of individual femoral or tibial samples used for preparation of RNA and subsequent QPCR assays.

Therapeutic hyaluronan and bone remodeling in osteoarthritis

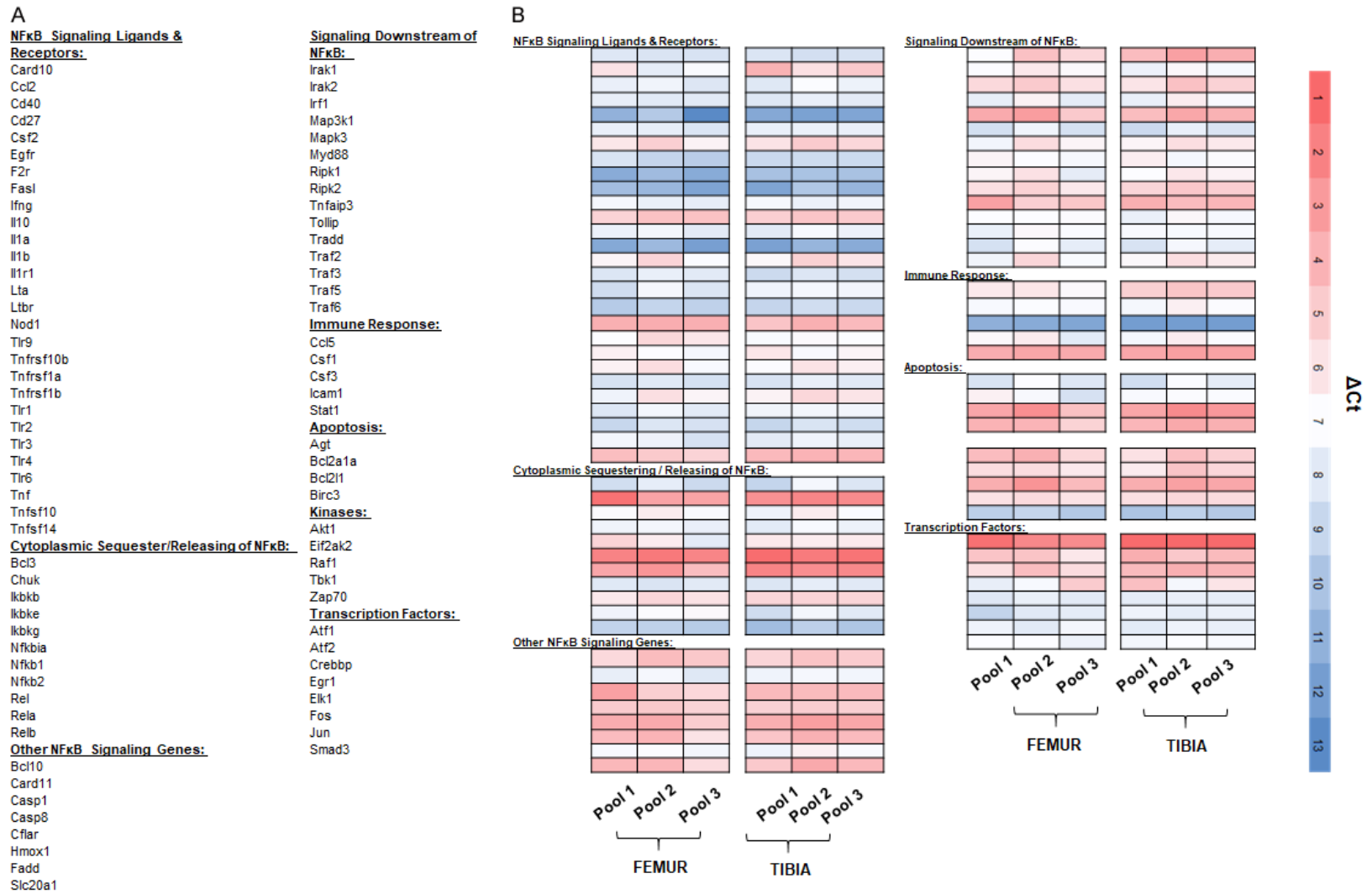


Figure S1. A. List of Genes included on the Nfkb Pathway Array Plate. B. Gene Expression (ΔC_t) in Naïve Femoral and Tibial Epiphyses showing reproducibility between pools.

Therapeutic hyaluronan and bone remodeling in osteoarthritis

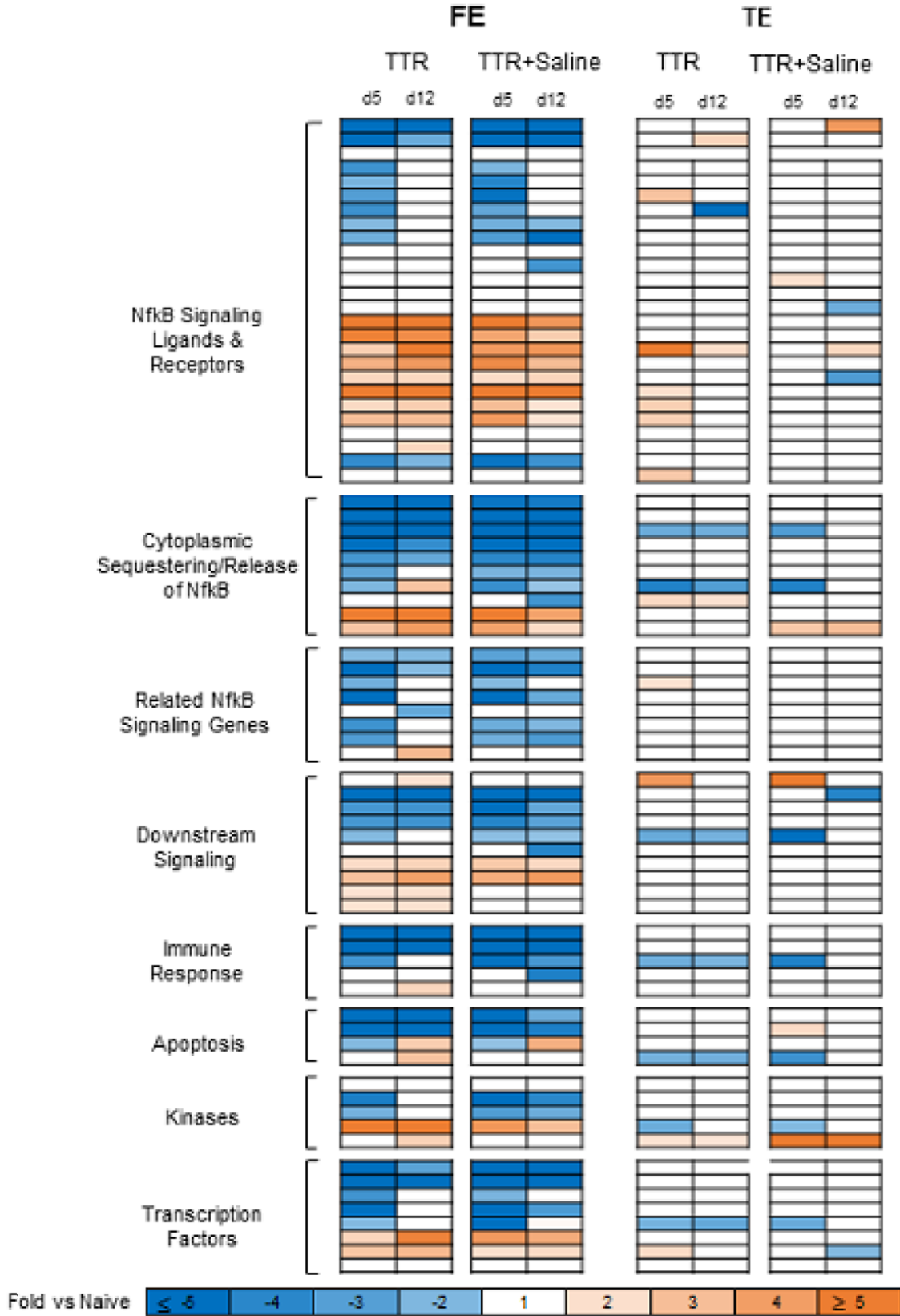


Figure S2. Heatmap Illustration of fold changes vs UI in relative mRNA abundance for Nfkb Pathway genes in femoral and tibial epiphyses in the TTR model without and with IA Saline. Colored boxes are only shown for statistically significant ($p < 0.05$) fold changes relative to naïve levels.

Therapeutic hyaluronan and bone remodeling in osteoarthritis

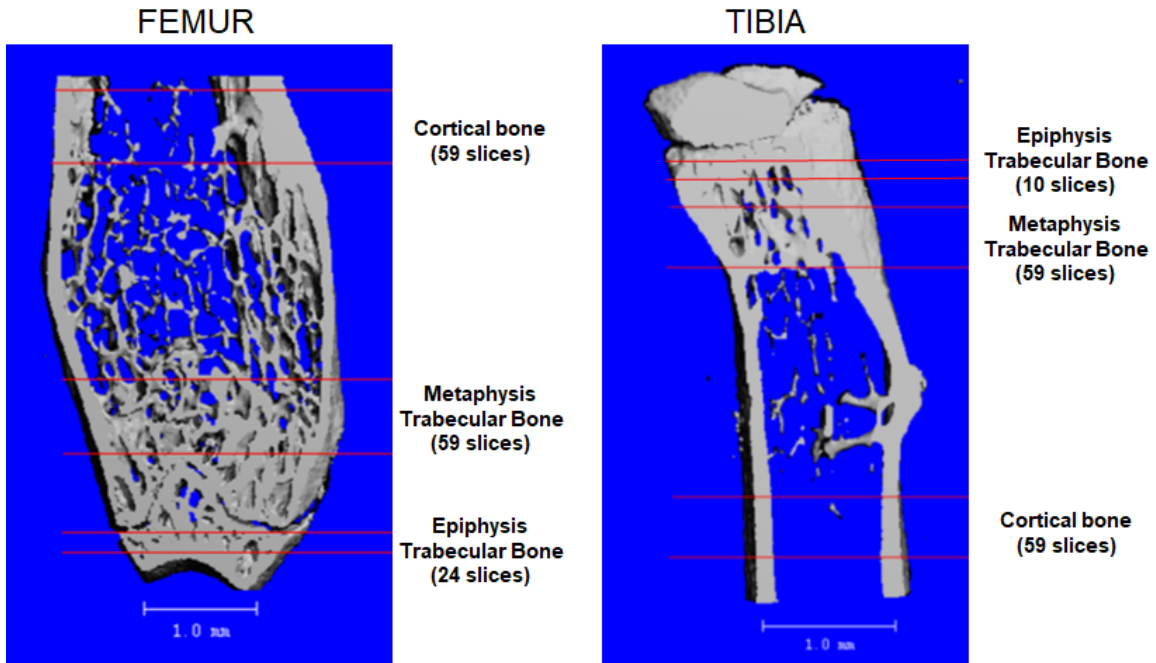


Figure S3. ROIs for quantitation of bone structural parameters.

Table S2. Metaphyseal and Cortical Bone Properties of two different sets of UI 16 week old mice, maintained at cage activity

Compartment	Parameter	Set 1 (n=4) Mean (S.D.)	Set 2 (n=4) Mean (S.D.)	
FEMUR	BV/TV	0.07 (0.014)	0.23 (0.044)	
	Tb N	4.41 (0.239)	5.92 (0.366)	
	Metaphyses	Tb Th (mm)	0.04 (0.006)	0.05 (0.005)
		Tb Sp (mm)	0.23 (0.024)	0.16 (0.012)
TIBIA	BV/TV	0.12 (0.003)	0.22 (0.050)	
	Tb N	5.00 (0.209)	5.93 (0.671)	
	Metaphyses	Tb Th (mm)	0.04 (0.001)	0.05 (0.003)
		Tb Sp (mm)	0.20 (0.009)	0.16 (0.023)
FEMUR	Cortical Bone	BV/TV	0.98 (0.01)	0.96 (0.016)
TIBIA			0.95 (0.085)	1.05 (0.021)

Therapeutic hyaluronan and bone remodeling in osteoarthritis

Table S3. Fold Changes in Nfkb Pathways genes (p≤0.05) of IA HA vs TTR Only

GENE	FEMUR								TIBIA													
	INJECTED				CONTRA				INJECTED				CONTRA									
	d 5	d 12	d 19	d 26	GENE	d 5	d 12	d 19	d 26	GENE	d 5	d 12	d 19	d 26	GENE	d 5	d 12	d 19	d 26	GENE	d 5	d 12
<i>Casp8</i>	11.3	-8.69	2.51		<i>Irak2</i>	-4.24	3.08			<i>Akt1</i>	2.24	2.09			<i>Jun</i>	2.55	2.25			<i>Agt</i>	10.10	3.17
<i>Bcl2l1</i>	7.80	-6.28			<i>Lta</i>	-4.84	5.93			<i>Relb</i>	-2.11	2.78			<i>Zap70</i>	2.16				<i>Akt1</i>	3.76	
<i>Bcl2a1a</i>	6.62	-9.62			<i>Ltbr</i>	-10.9	3.53			<i>Lta</i>	-2.18	2.06	3.32		<i>Bcl3</i>	2.16		1.98		<i>Atf1</i>	3.03	
<i>Bcl10</i>	6.11	-11.71	2.37		<i>Map3k1</i>	-12.9				<i>Csf2</i>	-58.7	5.17	5.34	-2.97	<i>Il1b</i>	1.98	-2.25			<i>Atf2</i>	2.93	
<i>Csf3</i>	5.81				<i>Mapk3</i>	-2.75	3.56			<i>Agt</i>				3.43	<i>Agt</i>	-2.00			2.21	<i>Bcl10</i>	2.24	
<i>Crebbp</i>	5.09	-9.52	2.15		<i>Myd88</i>		2.35			<i>Atf1</i>				-2.21	<i>Relb</i>	-41.4				<i>Bcl2a1a</i>	2.21	
<i>Jun</i>	4.94	-5.90	2.22		<i>Nfkb1</i>		4.01			<i>Bcl3</i>		2.58	2.09	2.28	<i>Lta</i>		-3.13		-62.6	<i>Bcl2l1</i>	2.19	
<i>Card10</i>	4.71	-21.7			<i>Nfkb2</i>		2.24			<i>Card10</i>			2.11		<i>Casp8</i>		-1.89			<i>Bcl3</i>	2.11	
<i>Atf1</i>	4.63	-8.09			<i>Nfkbia</i>		2.28			<i>Casp1</i>				-2.61	<i>Ccl2</i>				-4.86	<i>Birc3</i>	2.02	
<i>Fasl</i>	4.55	-6.84	2.67		<i>Nod1</i>		3.39			<i>Ccl2</i>		-2.92		-12.77	<i>Csf2</i>		2.02			<i>Card10</i>	-3.94	
<i>Bcl3</i>	4.55	-27.9			<i>Raf1</i>		3.84			<i>Chuk</i>				-2.13	<i>Csf3</i>			-2.27		<i>Egfr</i>		
<i>Birc3</i>	4.42	-11.1			<i>Rel</i>	-3.63	3.97			<i>Csf3</i>		8.22	2.35		<i>Egfr</i>		2.45			<i>Il1b</i>		
<i>Chuk</i>	3.71				<i>Rela</i>	-3.99	4.29			<i>Egr1</i>				-2.78	<i>Egr1</i>				-2.57	<i>Raf1</i>		
<i>Atf2</i>	3.59	-8.30	3.17		<i>Relb</i>	-7.84				<i>Fos</i>				3.91	<i>Ikake</i>							
<i>Agt</i>	3.52	-20.9			<i>Ripk1</i>	-4.05				<i>lfng</i>				11.5	<i>Il10</i>		-3.58	-4.35	-2.31			
<i>Eif2ak2</i>	3.30	-3.44	6.36	2.00	<i>Ripk2</i>	-2.54				<i>Ikake</i>				2.31	<i>Tlr9</i>				2.00			
<i>Il1a</i>	2.77		3.55		<i>Slc20a1</i>	-2.38	2.09			<i>Ikake</i>				-2.14	<i>Tnfrsf1a</i>		2.16					
<i>Card11</i>	2.58	-23.0			<i>Smad3</i>		2.99			<i>Il10</i>				3.54								
<i>lfng</i>	2.56	-12.2			<i>Stat1</i>		4.70			<i>Il1a</i>				2.18								-2.36
<i>lrf1</i>	2.45	-4.37	3.85		<i>Tbk1</i>		2.38			<i>Il1b</i>				2.61								
<i>Akt1</i>	2.38	-10.2	3.33		<i>Tlr1</i>		2.16			<i>Ltbr</i>												2.01
<i>Ikake</i>	2.37	-20.0	2.19		<i>Tlr2</i>		2.83			<i>Myd88</i>												
<i>Cd40</i>	2.35	-8.01			<i>Tlr3</i>		2.28			<i>Nfkb2</i>				2.39								2.10
<i>Ccl2</i>	2.24	-12.7	2.13	-2.92	<i>Tlr4</i>			2.22		<i>Raf1</i>												
<i>Ccl5</i>	2.08	-6.80	2.93		<i>Tlr6</i>		2.78			<i>Rela</i>												2.75
<i>Hmox1</i>	2.06	-13.1			<i>Tlr9</i>		2.16			<i>Tlr2</i>				2.13								
<i>Fos</i>	2.03	-3.27			<i>Tnf</i>		2.88			<i>Tlr4</i>												2.01
<i>Cd27</i>	2.00	-6.91	2.88		<i>Tnfaip3</i>		1.94			<i>Tlr6</i>												2.25
<i>Casp1</i>		-19.2			<i>Tnfrsf1a</i>		2.39			<i>Tnf</i>												2.65
<i>Cflar</i>		-6.42	2.21		<i>Tnfrsf1b</i>		3.32			<i>Tnfrsf10b</i>				6.72								2.27
<i>Csf1</i>		-16.2			<i>Tnfsf10</i>		2.20			<i>Tnfrsf10b</i>												2.58
<i>Egfr</i>		-14.2	2.09		<i>Tollip</i>		2.24			<i>Tnfrsf1a</i>												2.72
<i>Egr1</i>		-14.7								<i>Tnfrsf1b</i>												-2.59
<i>Elk1</i>		-4.04	2.77							<i>Tradd</i>												2.22
<i>F2r</i>		-4.45	4.95	2.62						<i>Traf5</i>												2.09
<i>Fadd</i>		-6.23								<i>Traf6</i>				4.49								
<i>Icam1</i>		-14.5	2.45							<i>Zap7</i>												
<i>Ikake</i>		-10.1																				
<i>Ikake</i>		-4.10	2.03																			
<i>Il1b</i>			2.81																			
<i>Il1r1</i>			3.79																			
<i>Irak1</i>			3.58																			

Therapeutic hyaluronan and bone remodeling in osteoarthritis

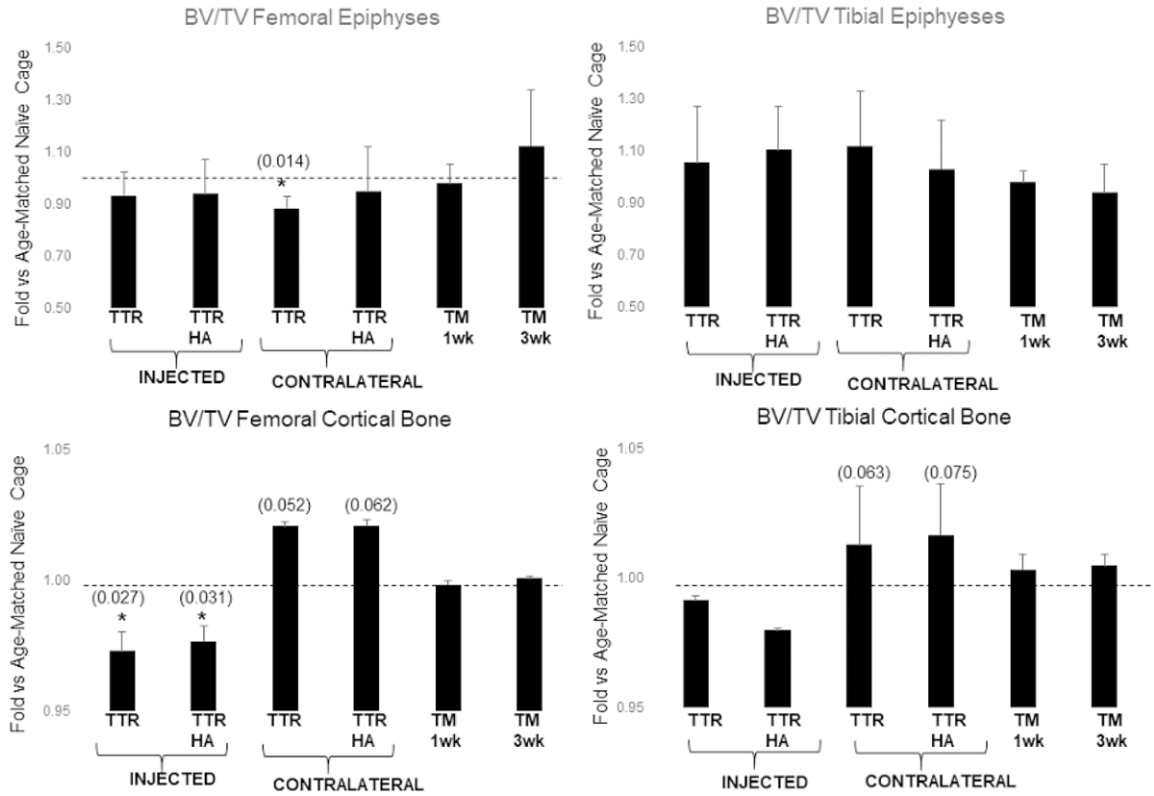


Figure S4. Changes in Epiphyseal and cortical BV/TV after TTR, TTR+HA and TM treatments. Injected and Contralateral legs were analysed separately for the TTR or TTR+HA groups. Data are expressed relative to UI (for TTR \pm HA) or Cage (for TM) age matched controls. Injected and Contralateral legs were analysed separately for the TTR or TTR+HA groups.

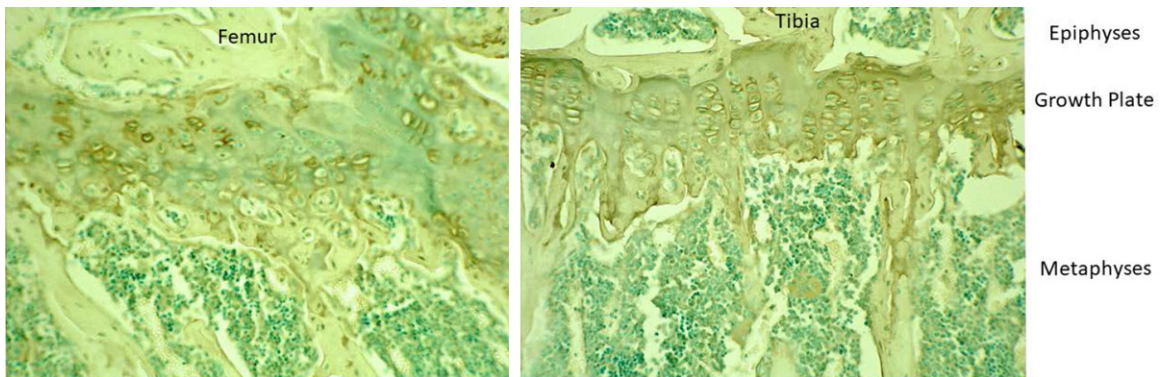


Figure S5. Non-Immune Controls for NOS2 and Arginase 1 IHC.

Therapeutic hyaluronan and bone remodeling in osteoarthritis

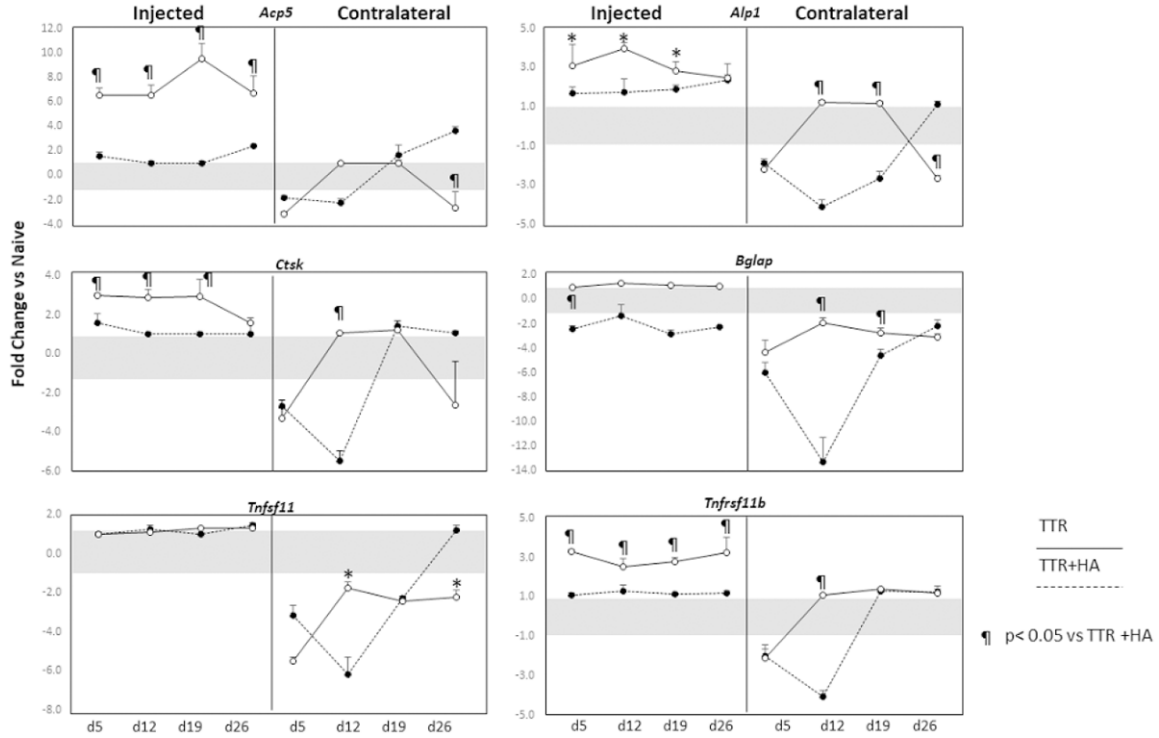


Figure S6. Effect of TTR (●) and TTR+HA (○) on fold changes (vs naïve) in expression of Bone Metabolism Genes in the Femoral Compartment.

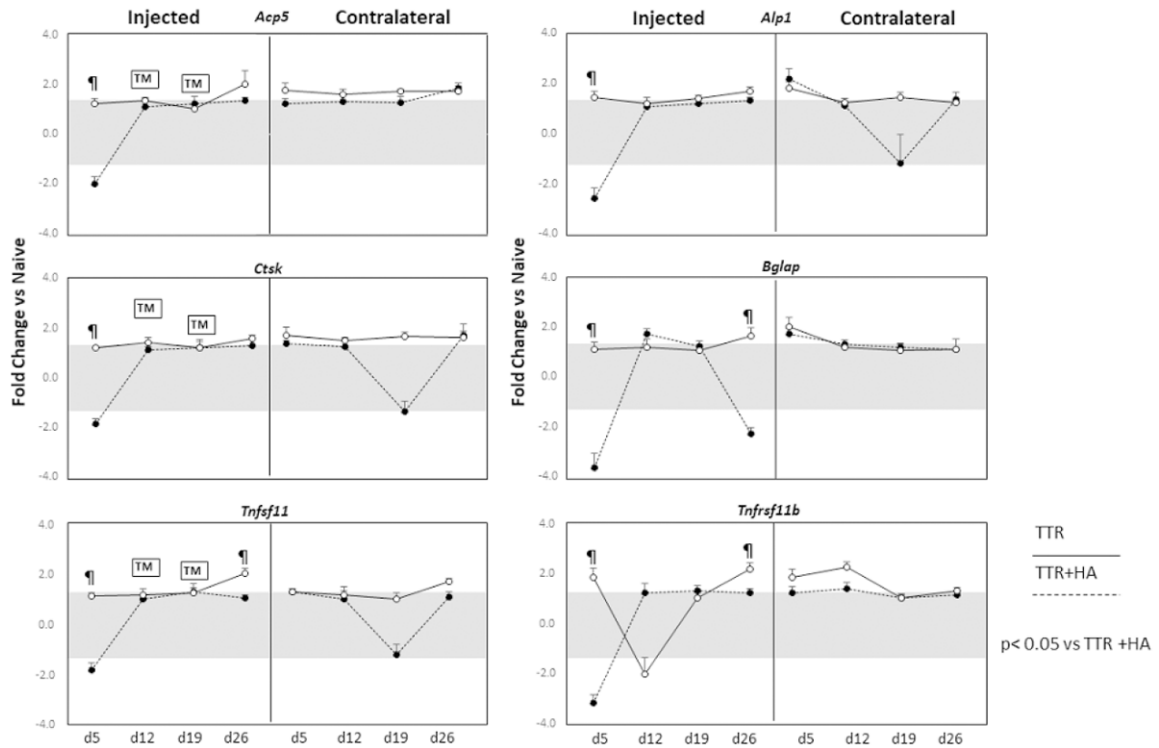


Figure S7. Effect of TTR (●) and TTR+HA (○) on fold changes (vs naïve) in expression of Bone Metabolism Genes in the Tibial Compartment.